Journal of Controlled Release 302 (2019) 63–78

Contents lists available at ScienceDirect

Journal of Controlled Release

journal homepage: www.elsevier.com/locate/jconrel

Modulation of pericytes by a fusion protein comprising of a PDGFRβ-antagonistic affibody and TNFα induces tumor vessel normalization and improves chemotherapy

Qing Fan[a,1], Ze Tao[a,1], Hao Yang[a], Qiuxiao Shi[a], Hong Wang[b], Dianlong Jia[a,2], Lin Wan[a], Jie Zhang[a], Jingqiu Cheng[a,*], Xiaofeng Lu[a,*]

[a] Key Lab of Transplant Engineering and Immunology, MOH, Regenerative Medical Research Center, West China Hospital, Sichuan University, Chengdu 610041, China
[b] Department of Ultrasound, West China Hospital, Sichuan University, Chengdu 610041, China

ARTICLE INFO

Keywords:
Vessel normalization
Cancer-targeted therapy
Pericytes
Tumor necrosis factor α
Affibody

ABSTRACT

The delivery of anticancer drugs is hampered by tumor vessels with abnormal structure and function, which requires that vessel normalization be mediated by pharmaceutics. The current strategies for vessel normalization focus on direct modulation of endothelial cells (ECs), which frequently affect vessels in normal tissues. Modulating EC-supporting cells, such as pericytes (PCs), is a new direction. Here, we produced a fusion protein, *Z*-TNFα, by fusing the platelet-derived growth factor receptor β (PDGFRβ)- antagonistic affibody $Z_{PDGFRβ}$ to tumor necrosis factor α (TNFα). Owing to the affinity of fused $Z_{PDGFRβ}$ for PDGFRβ, *Z*-TNFα binds PDGFRβ$^+$ PCs but not PDGFRβ$^-$ ECs. Low-dose (1 μg/mouse) *Z*-TNFα treatment remodeled the tumor vessels, thus reducing vessel permeability and increasing vessel perfusion. As a result, the *Z*-TNFα treatment improved the delivery of doxorubicin (DOX) and enhanced its antitumor effect, indicating that *Z*-TNFα induced normalization of tumor vessels. Mechanically, the tumor vessel normalization mediated by Z-TNFα might be attributed to the reduction of vascular endothelial growth factor (VEGF) secretion by PCs and the elevated expression of intercellular cell adhesion molecule-1 (ICAM-1) in PCs, which might suppress the proliferation and migration of ECs and simultaneously trigger interaction between perivascular macrophages and PCs. These results demonstrated that tumor-associated PCs could be considered novel target cells for vessel normalization, and *Z*-TNFα might be developed as a potential tool for antitumor combination therapy.

1. Introduction

Excessive blood vessel formation is a hallmark of rapidly growing tumors. However, these tumor vessels are frequently abnormal in structure and function [1,2]. Compared to normal vessels, tumor vessels are immature and have structural abnormalities, such as dilation, tortuosity, and inadequate perivascular cell investment [3]. It is known that the endothelium of tumor vessels consists of irregularly lined endothelial cells (ECs) covered with a limited number of pericytes (PCs) and smooth muscle cells (SMCs). In addition, the basic membranes are usually lacking in the wall of tumor vessels. These abnormalities in structure make tumor vessels hyperpermeable to protein-rich tissue fluids. Due to the disabled lymphatic drainage of tumor tissues, the fluids leaked into extravascular tissues induce high interstitial fluid pressure (IFP), which impairs the tumor vessel perfusion and results in inefficient blood supply. To obtain more nutrients and oxygen, tumors produce excessive proangiogenic factors, thus inducing an endless self-reinforcing loop of angiogenesis, which produces a hypoperfused vascular network with impeded drug delivery function. Systemic chemotherapy is seriously hampered by inefficient drug delivery in hypoperfused tumors [4,5].

Interestingly, it was reported that antiangiogenesis therapy ameliorated the efficacy of chemotherapy [6] as well as radiotherapy [7]. In the case of radiotherapy, the enhancement of treatment efficacy that is tissue oxygenation-dependent suggested that antiangiogenic therapy improved oxygen delivery in tumors. Further studies revealed that antiangiogenic therapy reduced vascular density and increased the PC coverage, which reduced the hypoxia and permeability, but improved

* Corresponding authors.
E-mail addresses: jqcheng@scu.edu.cn (J. Cheng), xiaofenglu@scu.edu.cn (X. Lu).
[1] These authors contributed equally to this work.
[2] Present address: College of Pharmacy, Liaocheng University, Liaocheng, Shandong, 252,000, China.

https://doi.org/10.1016/j.jconrel.2019.03.018
Received 11 September 2018; Received in revised form 19 March 2019; Accepted 21 March 2019
Available online 28 March 2019
0168-3659/

the perfusion of tumor vessels [8]. Antiangiogenic therapy made tumor vessels similar to normal vessels in structure and function, which was designated as “vessel normalization” by Rakesh K. Jain in 2001 [9]. Although not as good as that of normal vessels, the perfusion and drug delivery of tumor vessels administered antiangiogenic therapy are much better than those of untreated tumor vessels. Consequently, vessel normalization has been considered as a novel paradigm for combination strategy to overcome the resistance of hypoperfused tumors to conventional chemotherapy and radiotherapy [2,3,8].

Vessel sprouting is initiated by the differentiation of ECs into specialized tip and stalk cells, which triggers extensive proliferation of ECs during tumor angiogenesis. In fact, in rapidly growing tumors, the proliferation rate of ECs was approximately 50–200 times higher than that of normal quiescent ECs [10]. Inhibition of the proliferation and migration of ECs by targeting the vascular endothelial growth factor (VEGF)/VEGF receptor (VEGFR) [11] and the ANG2/TIE2 [12] axes or downregulating the metabolism of ECs [13] promoted normalization of tumor vessels. In addition, immune cells are also involved in angiogenesis. Although the underlying mechanism is unclear, the interaction between immune cells [14,15] and vascular cells has been shown to contribute to tumor vessel normalization. However, owing to the lack of adhesion molecules in anergic tumor vascular cells, the recruitment of immune cells into the tumor is usually impeded [16]. However, treatment with low-dose EC-targeted cytokines, such as tumor necrosis factor α (TNFα) [17–19] and LIGHT [20,21], could induce adhesion molecule expression and recruitment of immune cells to promote tumor vessel normalization. One EC-targeted TNFα agent, NGR-TNFα, has entered phase II/III clinical trials for combination therapy for advanced cancers [22]. These results demonstrated that ECs were key target cells for tumor vessel normalization. However, direct modulation of tumor-associated ECs frequently affects the vessels in normal tissue during extended therapy, and modulating EC-supporting cells might be better for tumor vessel normalization [23].

ECs and PCs are major vascular cells in tumor vessels. ECs comprise the inner lining of vessels whereas PCs encompass the endothelium. The crosstalk between PCs and ECs regulates the contractility, stabilization and permeability of blood vessels. It is known that ECs in the angiogenic sprouts could produce platelet-derived growth factor-BB (PDGF-BB) to stimulate the proliferation and migration of platelet-derived growth factor receptor β (PDGFRβ)-expressing PCs. In addition, PDGF-BB could stimulate PCs to produce VEGF, which can drive the proliferation and migration of ECs and potentiate angiogenesis. These results demonstrate that the PDGF-BB/PDGFRβ pathway mediates the crosstalk between PCs and ECs and play important roles in proangiogenesis [24]. Interrupting the PC-EC crosstalk with PDGFRβ inhibitors reduced angiogenesis in tumors [25], suggesting that PDGFRβ-expressing PCs might be considered as novel target cells for vessel normalization. Recently, numerous affibodies that specifically bind PDGFRβ (designated as $Z_{PDGFRβ}$) with high affinity (nM) had been identified by Lindborg et al. [26]. These affibodies could inhibit the phosphorylation of PDGFRβ [26], suggesting that it might reduce angiogenesis by interrupting the PC-EC crosstalk. In addition, EC-targeted TNFα promoted tumor vessel normalization by launching the interaction between immune cells and vascular cells [17,18]. These results triggered our interest to investigate whether $Z_{PDGFRβ}$-directed TNFα could promote vessel normalization by dual mechanisms, including reducing VEGF production by PCs and recruiting immune cells to the tumor vessels.

In this experiment, $Z_{PDGFRβ}$ was fused to the N-terminus of mouse TNFα to produce a fusion protein, *Z*-TNFα. Subsequently, the receptor and cell binding of Z-TNFα were measured, followed by analysis of the impact of *Z*-TNFα treatment on proliferation and migration, VEGF production, and adhesion molecule expression in PCs. Finally, after evaluation of the *Z*-TNFα-induced modifications of tumor vessels in structure and function, the antitumor effect of Z-TNFα as a monotherapy or in combination with doxorubicin (DOX) was examined in mouse bearing tumor grafts.

2. Materials and methods

2.1. Expression and purification of proteins

$Z_{PDGFRβ}$ was prepared according to our previous description [27]. To produce the fusion protein *Z*-TNFα, $Z_{PDGFRβ}$ was fused to the N-terminus of mouse TNFα (77-233aa) with a flexible linker $(G4S)_3$. The gene encoding *Z*-TNFα was synthesized by GenScript (Nanjing, China) and cloned into the pQE30 plasmid at BamHI and *Sal*I to construct pQE30-Z-TNFα. Similarly, pQE30-TNFα was constructed by inserting the gene encoding TNFα into the pQE30 plasmid. The expression plasmid was transformed into *E. coli* M15 and induced with isopropyl-L-thio-β-D-galactopyranoside (IPTG, 0.05 mM) overnight at 26 °C. Subsequently, the cells were collected by centrifugation at 7000*g* at 4 °C and resuspended in lysis buffer (50 mM phosphate, pH 8.0, 300 mM NaCl, 20 mM imidazole, and 10 mM β-mercaptoethanol). After sonication on ice, the recombinant proteins in the supernatant were recovered using Ni-NTA affinity chromatography according to the manual provided by the manufacturer. The purified proteins were dialyzed against phosphate-buffered saline (PBS, 8 g/L NaCl, 0.2 g/L KCl, 3.49 g/L $Na_2HPO_4{\cdot}12H_2O$, and 0.2 g/L KH_2PO_4) overnight at 4 °C followed by analysis with sodium dodecyl sulfate-polyacrylamide gel electrophoresis (SDS-PAGE) and size-exclusion chromatography (Superdex G75 Increase 10/30 column, GE Healthcare, CA, USA). The protein concentrations were measured using a DC protein assay kit (Bio-Rad, CA, USA).

2.2. In vitro protein binding assays

To examine the binding of $Z_{PDGFRβ}$ to PDGFRβ, the PDGFRβ-Fc fusion proteins (R&D, MN, USA) were immobilized onto a COOH-sensor chip. Subsequently, a solution containing different concentrations of $Z_{PDGFRβ}$ was introduced into the chip followed by surface plasmon resonance analysis performed on an OpenSPR system (Nicoya Lifesciences Inc., Kitchener, Canada) [28]. The biolayer interferometry performed on a BlItz® System (Pall ForteBio LLC, CA, USA) was used for the binding assay of *Z*-TNFα and TNFα to PDGFRβ or TNFα receptors (TNF receptor 1, TNFR1; TNF receptor 2, TNFR2). PDGFRβ-Fc, TNFR1-Fc or TNFR2-Fc fusion proteins were immobilized onto a protein A-coated probe followed by the insertion into a solution containing different concentrations of *Z*-TNFα or TNFα for the association and disassociation analysis. The kinetic constants, including the association constant (ka), dissociation constant (kd) and affinity (KD, KD = kd/ka), were calculated using a software according to a 1:1 binding model.

2.3. Cell culture

B16F1 melanoma cells, S180 sarcoma cells, ECs and SMCs were purchased from the American Type Culture Collection (ATCC, VA, USA). These cells were cultured in Dulbecco's-modified Eagle's medium (DMEM) supplemented with 10% fetal bovine serum, 2 mM L-glutamine, 100 U/ml penicillin, and 100 μg/ml streptomycin. Pericytes (PCs) derived from human brain vasculature were purchased from ScienCell (CA, USA) and cultured in their specific medium. All cells were cultured at 37 °C in a 5% CO_2 humidified atmosphere.

2.4. Cytotoxicity assays

Approximately, 1×10^4 cells were inoculated in a 96-well plate and cultured overnight followed by treatment with $Z_{PDGFRβ}$, *Z*-TNFα, TNFα or doxorubicin (DOX) as a single agent or in combination. To examine the cytotoxicity of Z-TNFα or TNFα in combination with DOX, the protein was added into the cells 2 h prior to the addition of DOX. After treatment overnight, the surviving cells were measured using the Cell Counting Kit-8 (CCK-8, Dojindo, Japan). The viability of the cells treated with PBS was considered 100%.

2.5. Cell proliferation and migration assays

For the PC proliferation assays, 8×10^3 cells were inoculated in a 96-well plate and starved in a PC-specific medium containing 0.5% fetal bovine serum overnight. Subsequently, cells were pretreated with 400 nM $Z_{PDGFR\beta}$, *Z*-TNFα, TNFα or PBS for 1 h at 37 °C followed by the addition of PDGF-BB (50 ng/ml). The surviving cells were measured using CCK-8 24 h later. The viability of cells treated with PBS in the absence of PDGF-BB was considered to be 100%. Compared to the viability of cells treated with PBS in the presence of PDGF-BB, the reduced cell viability reflects the proliferation inhibition mediated by the proteins.

To evaluate the inhibition of the proteins on the migration of PCs, wound-healing experiments were performed according to Xi et al. [29]. Briefly, 5×10^4 PCs were inoculated in a 24-well plate and starved overnight. The cell monolayer was scratched using a 1 ml pipette tip. After three washes with PBS, the cells were pretreated with 200 nM $Z_{PDGFR\beta}$, *Z*-TNFα or TNFα for 1 h at 37 °C followed by the addition of PDGF-BB (50 ng/ml) into the cells. The scratches were photographed at 0 and 24 h post-treatment. The wound-healing of PCs treated with PBS in the absence or in the presence of PDGF-BB was used as positive and negative controls, respectively.

2.6. ELISA assays

VEGF produced by PCs was measured using a VEGF ELISA kit (DLDEVELOP, Wuxi, China). Approximately, 1×10^4 PCs were inoculated in a 96-well plate and starved overnight. The cells were pretreated with 2.5 nM $Z_{PDGFR\beta}$, *Z*-TNFα or TNFα for 1 h at 37 °C prior to the addition of PDGF-BB (50 ng/ml). After incubation for 24 h, the culture supernatant was collected for the ELISA assays. The cells treated with PBS in the absence and in the presence of PDGF-BB were used as negative and positive controls, respectively.

2.7. Flow cytometry

To detect the expression of PDGFRβ, neuron-glia antigen 2 (NG2) and alpha-smooth muscle actin (α-SMA), antibodies (rabbit anti-human PDGFRβ, NG2 or α-SMA, Abcam, MA, USA) were incubated with the cells (3×10^5 cells in 100 μl of PBS) at room temperature for 1.5 h. After three washes with PBS containing 0.5% fetal bovine serum, the cells were incubated with the secondary antibody (donkey anti-rabbit IgG DyLight 488, Abcam, MA, USA) for 0.5 h at room temperature. Finally, the cells were washed three times with PBS containing 0.5% fetal bovine serum prior to the flow cytometry analysis. For the cell binding assays, $Z_{PDGFR\beta}$, TNFα and *Z*-TNFα were labeled with 5(6)-carboxyfluorescein (FAM) (Sigma, MA, USA) according to Wei et al. [30]. Approximately, 2×10^5 cells were incubated with FAM-labeled proteins at room temperature for 1 h followed by three washes with PBS and analysis on a flow cytometer (Cytomics FC 500, Beckman Coulter, CA, USA). To investigate the PDGFRβ-dependent binding, PCs were preincubated with the anti-PDGFRβ antibody at room temperature for 1 h prior to the incubation with FAM-labeled proteins. The reduction in binding rate reflects the role of the receptor in mediating PC binding to proteins.

To detect the inducible expression of intercellular cell adhesion molecule-1 (ICAM-1) in PCs, the cultured cells were treated with TNFα or *Z*-TNFα (40 nM) for 1.5 h on ice immediately after detachment. Subsequently, the cells (1×10^5 cells/well) were washed with PBS followed by further culture in 6-well plates coated with rat-tail collagen type I. Approximately 24 h later, these cells were collected for analysis of the expression of ICAM-1 with the mouse anti-human ICAM-1 antibody (Biolegend, CA, USA).

2.8. Optical imaging

Optical imaging was performed according to Shi et al. [31]. Briefly, $Z_{PDGFR\beta}$ was labeled with CF™ 750 succinimidyl ester. S180 sarcoma cells (2×10^6 cells/mouse) were subcutaneously implanted into female ICR mice ($n = 3$, 16–18 g). The longitudinal (L) and transverse (W) diameters of the tumor grafts were recorded every day to calculate the tumor volumes (V) by the following formula: $V = L \times W^2/2$. When the tumor volume reached 100–200 mm^3, the mice were intravenously injected with CF750-labeled $Z_{PDGFR\beta}$ (70 μg/mouse) followed by dynamic scanning using the SPECTRAL Lago and Lago X Imaging Systems (Spectral, AZ, USA). At the end of the experiment, the mice were sacrificed. The tumor grafts and some normal organs/tissues were collected and scanned. Accumulation of $Z_{PDGFR\beta}$ in tumor grafts reflects the tumor-homing of $Z_{PDGFR\beta}$.

2.9. Structure and function evaluation of tumor vessel

To visualize the tumor-associated cells, tumor grafts from mice were sectioned into 5 μm or 100 μm sections under frozen conditions. After fixation with paraformaldehyde (PFA), the tumor tissues were incubated with primary antibodies against CD31, PDGFRβ, NG2, α-SMA or CD68 (37 °C, 1.5 h for 5 μm sections; 4 °C overnight for 100 μm sections) followed by the incubation with corresponding secondary antibodies at 37 °C for 0.5–1.5 h. The primary antibodies included rat anti-mouse CD31 (Biolegend, CA, USA), rabbit anti-mouse PDGFRβ, rabbit anti-mouse α-SMA, rabbit anti-mouse CD68 (Abcam, CA, USA), and rabbit anti-mouse NG2 (Millipore, MA, USA). The secondary antibodies were goat anti-rat IgG (DyLight 550) and donkey anti-rabbit IgG (DyLight 488). The nuclei of the cells were stained with DAPI. To localize the recombinant proteins on the PDGFRβ-expressing cells in tumors, mice bearing tumor grafts were intravenously injected with FAM-labeled proteins. Subsequently, tumor grafts were removed at 1 h post-injection followed by sectioning and staining with an antibody against PDGFRβ.

To investigate the role of *Z*-TNFα in prompting tumor vessel normalization, 5×10^4 B16F1 melanoma cells were subcutaneously implanted into C57BL/6 mice. From day 6 post-inoculation, mice were intravenously injected with 1 μg of Z-TNFα every other day for a total of three injections. The mice in the control group were injected with the same volume of PBS. On the second day after the last injection, the structure and function of the tumor blood vessels were analyzed. The vascular perfusion assessment using fluorescein isothiocyanate (FITC)-labeled tomato lectin (Sigma, CA, USA) was performed according to the description by Maione et al. [32]. The tumor vascular perfusion was also evaluated by contrast-enhanced ultrasonography (CEUS) [33] performed using the PHLIPS IU22 ultrasound system (Philips, Best, Netherlands) equipped with a broadband 5–12 MHz L12–5 transducer. SonoVue was used as intravenous contrast agent. A video comprising CEUS imaging of tumor graft was recorded for at least 30 s at a low mechanical index of 0.07. Blood flow parameters including peak internsity (PI), area under the curve during wash-in (AUCwash-in), wash in slope, and time to peak intensity (TPI) were obtained by using QLAB software according to the time/intensity curve of each tumor graft ($n = 4$). To visualize the tumor vessel and blood flow in the tumor widow model, mice were intravenously injected with FITC-labeled dextran (70 kDa, Sigma, MA, USA, 1 mg/mouse) followed by observation the exposed tumor grafts under the confocal microscope (NiKON, A1RMP +). Moreover, leakage of FITC-labeled dextran was also used to evaluate the vascular permeability of tumor. The dextran remaining in the tumor tissues were observed under the confocal microscope after the mice were sequentially heart-perfused with PBS and 2% PFA under anesthesia at 10 min post-injection of dextran. To detect tumor hypoxia, Hypoxyprobe-1 was intravenously injected into the mice bearing tumor grafts at a dose of 60 mg/kg. After 1.5 h, the tumor grafts were removed and sectioned under frozen conditions followed by staining with a FITC-

labeled antibody against Hypoxyprobe-1 according to the instruction in the Hypoxyprobe-1 Plus kit (Millipore, MA, USA). To measure the tumor uptake of DOX, mice bearing tumor grafts were intravenously injected with 15 mg/kg DOX hydrochloride (Sigma, MA, USA). At 15, 45, or 90 min post-injection, the tumor grafts were removed and sectioned under frozen conditions. All the slides were observed under a fluorescence microscope or a confocal microscope. The fluorescence intensity was measured using the Image-J software or the Image-Pro Plus 6.0 software.

2.10. In vivo antitumor effect evaluation

Tumor-bearing animal models were constructed by subcutaneous injection of sarcoma S180 cells (2×10^6 cells/mouse) into female ICR mice or injection of melanoma B16F1 cells (5×10^4 cells/mouse) into female C57BL/6 mice. To evaluate the antitumor effects of *Z*-TNFα, mice ($n = 6$) bearing B16F1 tumor grafts were intravenously injected with a low-dose (1 μg/mouse) or high-dose (10 μg/mouse) of Z-TNFα every other day from day 5 post-inoculation. The mice in the control group were injected with the same volume of PBS. The tumor volumes were recorded every day and the tumor grafts were collected and weighed at the end of the experiment. The paraffin-sectioned tumor tissues were used for histological analysis by H&E staining.

To evaluate the antitumor effects of the combinational therapy of proteins and DOX, mice ($n = 6$) bearing S180 or B16F1 tumor grafts were intravenously injected with a low-dose (1 μg/mouse) *Z*-TNFα fusion protein or an equivalent mixture of $Z_{PDGFRβ}$ and TNFα followed by injection of different amounts (1–4 mg/kg) of DOX every other day. The mice in the control group were treated with PBS. The tumor volumes and body weights were recorded every day. At the end of the experiment, all tumor grafts were collected and weighted.

2.11. Acute toxicity assays

To evaluate the acute toxicity of high-dose (10 μg/mouse or more) TNFα proteins, C57BL/6 mice ($n = 10$, 16–18 g) were intravenously injected with TNFα (10 or 20 μg/mouse) or *Z*-TNFα (20 or 40 μg/mouse) every other day for at most three injections. The number of surviving mice was recorded every day. For the acute liver and kidney toxicity assessment of Z-TNFα, mice ($n = 6$, 16–18 g) were intravenously injected with 1 μg or 10 μg Z-TNFα every day for a total of 10 injections. The body weights of mice were recorded every day. Two days after the last injection, the mice were sacrificed. The blood samples were collected for measuring glutamic-pyruvic transaminase (ALT), glutamic-oxaloacetic transaminase (AST), uric acid (UA) and urea (UR). The histological examination of the liver and kidney was performed by H&E staining.

2.12. Statistical analysis

The one-way analysis of variance (ANOVA) test for multiple comparisons was performed using the SPSS software version 13.0. The results are expressed as the mean ± standard deviation (SD), and the significance level was defined as $p < .05$.

3. Results

3.1. PDGFRβ$^+$ cells in the mural of tumor blood vessels are predominantly pericytes

ECs form the endothelium in the wall of normal mature blood vessels, while PCs and SMCs form the mural, which serves to support and stabilize the endothelium. It is known that CD31 is an exclusive marker of ECs. Although PCs and SMCs express several biomarkers, none are exclusive. Consequently, the identification of these cells is dependent on both biomarkers and location along ECs [24]. Fig. 1A shows that PCs were PDGFRβ$^+$NG2$^+$α-SMA$^-$, whereas SMCs were PDGFRβ$^+$NG2$^-$α-SMA$^+$. In PDGFRβ$^+$ mural cells, NG2 and α-SMA might be considered exclusive markers for PCs and SMCs, respectively. Unlike the mature blood vessels, tumor blood vessels are usually immature with limited numbers of SMCs in the mural [34]. As shown in Fig. 1B, most PDGFRβ$^+$ cells were adjacent to CD31$^+$ ECs in the tumor grafts. Moreover, the distribution profile of PDGFRβ was identical to that of NG2, whereas few α-SMA$^+$ cells adjacent to ECs were observed (Fig. 1B). These results demonstrated that PDGFRβ$^+$ cells were predominantly PCs but not SMCs in the mural of tumor blood vessels.

3.2. Intravenously injected $Z_{PDGFRβ}$ binds PDGFRβ$^+$ pericytes and accumulates in tumor grafts

Recombinant $Z_{PDGFRβ}$ was produced by an *E. coli* expression system. As shown in Fig. 2A, the purified $Z_{PDGFRβ}$ was eluted as a single protein peak on the size exclusion chromatography column as well as visualized as a single protein band on the SDS-PAGE gel, indicating that $Z_{PDGFRβ}$ was purified to homogeneity. As shown in Fig. 2B, the surface plasmon resonance analysis demonstrated that $Z_{PDGFRβ}$ bound to PDGFRβ with an affinity of 4.5 nM. Flow cytometry indicated that the binding rate of $Z_{PDGFRβ}$ to PCs was higher than that of SMCs and ECs (Fig. 2C). Moreover, intravenously injected $Z_{PDGFRβ}$ was predominantly distributed to the PDGFRβ$^+$ cells in the tumor grafts (Fig. 2D). Further optical imaging revealed that $Z_{PDGFRβ}$ was enriched in tumor grafts with an intensity 2–6 times higher than that in other normal organs/tissues (Fig. 2E), indicating that $Z_{PDGFRβ}$ was tumor-homing. Since the PDGFRβ$^+$ cells in the mural of tumor vessels are predominantly PCs, these results suggested that $Z_{PDGFRβ}$ accumulates in the tumor grafts by binding to PCs.

3.3. Fusion to $Z_{PDGFRβ}$ endows TNFα with PDGFRβ-dependent pericyte-binding ability

To endow TNFα with PDGFRβ-binding ability, the $Z_{PDGFRβ}$ was fused to the N-terminus of TNFα to produce the fusion protein *Z*-TNFα. The purified Z-TNFα proteins were visualized as a single protein band on an SDS-PAGE gel (Fig. 3A) and eluted as a single protein peak from the column of size exclusion chromatography (Fig. 3B). These results demonstrated that the *Z*-TNFα proteins were purified to homogeneity. TNFα was also prepared by the same protocol. The protein-protein interaction analysis demonstrated that Z-TNFα bound PDGFRβ with a high affinity of 0.87 nM (Fig. 3C). In addition, *Z*-TNFα could bind PDGFRβ$^+$ PCs, and the PC binding rate of Z-TNFα was reduced from 80.3% to 18.6% by preincubating PCs with an antibody against PDGFRβ (Fig. 3D), indicating that the PC binding of *Z*-TNFα is PDGFRβ-dependent. However, TNFα alone could not bind PDGFRβ (Fig. 3C) and PDGFRβ$^+$ PCs (Fig. 3D). In addition, *Z*-TNFα showed low or no binding to other vascular cells (ECs and SMCs, Fig. S1A) and cancer cells (B16F1 and S180, Fig. S1B) expressing low levels of PDGFRβ. These results demonstrated that the fusion to $Z_{PDGFRβ}$ endowed TNFα with PDGFRβ-dependent pericyte-binding ability.

3.4. High-dose Z-TNFα suppresses tumor growth by disrupting blood vessels

Similar to TNFα, Z-TNFα could bind TNFα receptor 1 (TNFR1) and 2 (TNFR2). However, the affinities of *Z*-TNFα for TNFR1 and TNFR2 were 7.15 and 7.7 nM (Fig. S2B), respectively, compared to 6.4 and 6.6 of TNFα for TNFR1 and TNFR2 (Fig. S2A). These results suggested that the fusion to $Z_{PDGFRβ}$ slightly reduced the affinity of TNFα for its receptors. Accordingly, compared to TNFα, *Z*-TNFα showed reduced systemic toxicity. As shown in Fig. 4A, the first injection of 10 or 20 μg of TNFα caused 30% and 90% mouse mortality, respectively. After the third injection, the death rates of mice administered with 10 or 20 μg of TNFα were 60% and 100%, respectively. However, three injections of 40 μg of *Z*-TNFα only caused 20% mouse death. All mice administered

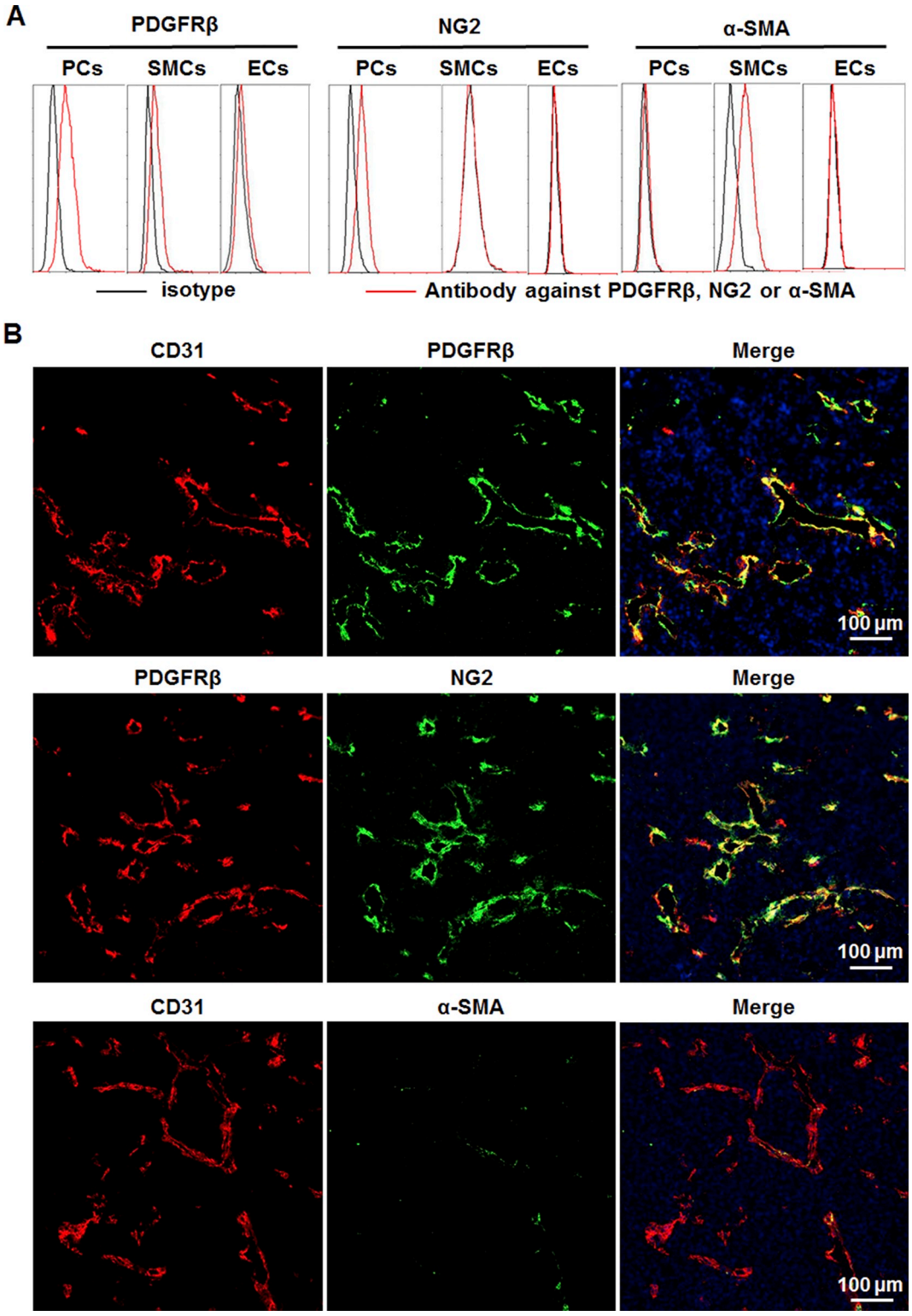

Fig. 1. Expression of PDGFRβ in tumor-associated pericytes. (A) Expression of PDGFRβ, NG2, and α-SMA in pericytes (PCs), smooth muscle cells (SMCs) and endothelial cells (ECs). Approximately, 3×10^5 cells were resuspended in 100 μl of PBS and incubated with the primary antibody at room temperature for 1.5 h followed by flow cytometry analysis. (B) Expression of PDGFRβ in the mural cells of tumor vessels. Tissues derived from B16F1 tumor grafts were sectioned under frozen conditions followed by colocalization analyses of PDGFRβ, NG2, or α-SMA with CD31 by immunofluorescence. The cell nuclei were visualized using DAPI (blue). (For interpretation of the references to colour in this figure legend, the reader is referred to the web version of this article.)

with 20 μg of *Z*-TNFα were alive after the third injection. These results demonstrated that the fusion to $Z_{PDGFR\beta}$ reduced the systemic toxicity of TNFα.

The fact that three injections of 20 μg of *Z*-TNFα did not cause death in mice triggered our interest in evaluating the direct antitumor effects of *Z*-TNFα. The mice were injected with a high-dose (10 μg/mouse) or low-dose (1 μg/mouse) of Z-TNFα every other day for a total of 5 injections. As shown in Fig. 4B, 10 μg of *Z*-TNFα showed promising tumor

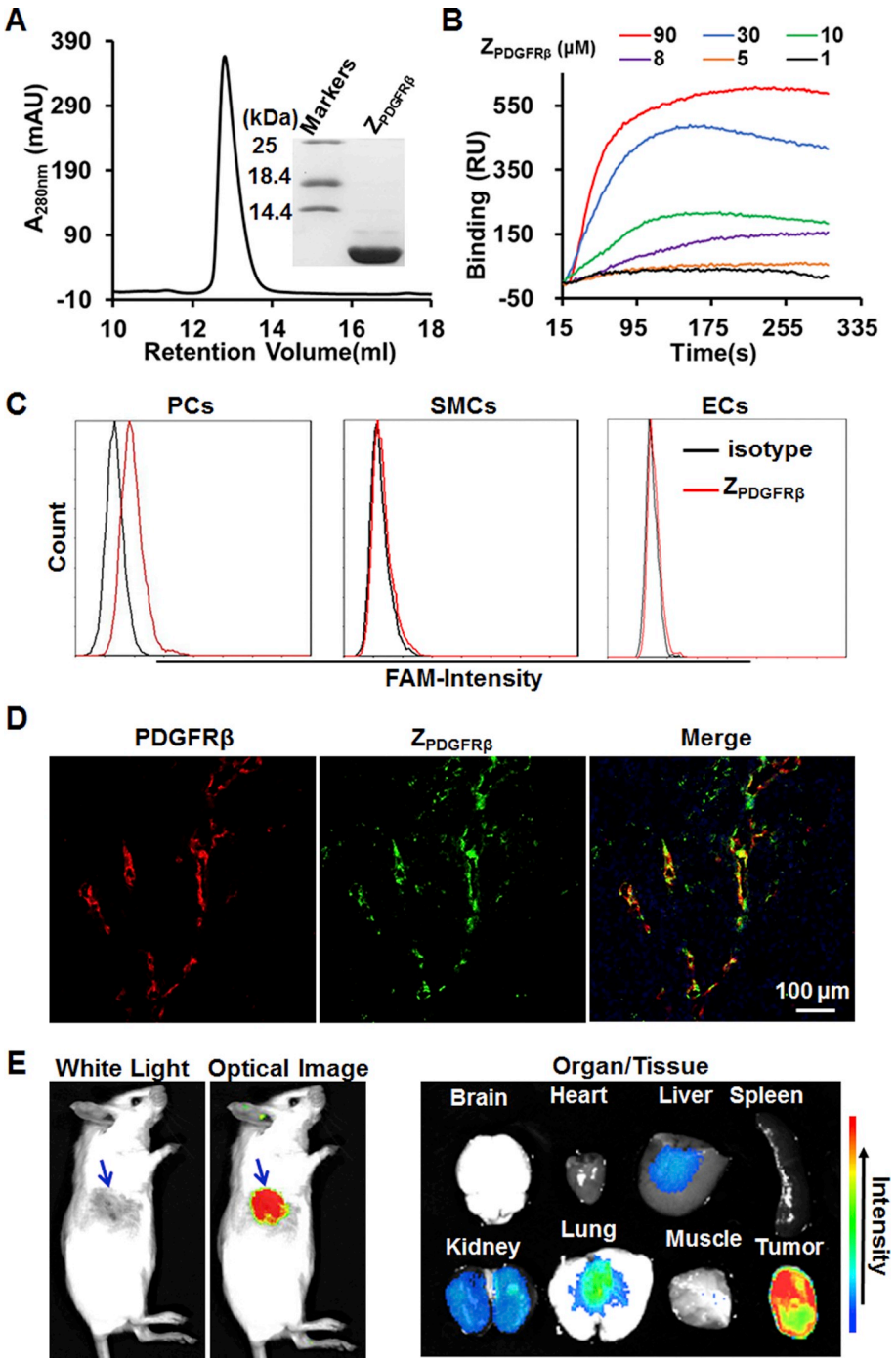

Fig. 2. Preparation and characterization of the $Z_{PDGFRβ}$ affibody ($Z_{PDGFRβ}$). (A) SDS-PAGE and size-exclusion chromatography of purified $Z_{PDGFRβ}$. (B) Binding of $Z_{PDGFRβ}$ to PDGFRβ. PDGFRβ-Fc was immobilized onto a COOH-sensor chip followed by introducing solutions containing different concentrations (1–90 μM) of $Z_{PDGFRβ}$ into the chip. The interaction between $Z_{PDGFRβ}$ and PDGFRβ-Fc was dynamically recorded and analyzed using the OpenSPR system. (C) Binding of $Z_{PDGFRβ}$ to PCs, SMCs, and ECs was analyzed by flow cytometry. (D) Localization of $Z_{PDGFRβ}$ in PDGFRβ$^+$ cells in B16F1 tumor tissues. Mice bearing B16F1 tumor grafts were intravenously injected with FAM-labeled $Z_{PDGFRβ}$ (70 μg/mouse, green). One hour later, the tumor grafts were removed and sectioned under frozen conditions followed by staining with an antibody against PDGFRβ (red). The nuclei of cells were visualized using DAPI (blue). (E) Tumor uptake of $Z_{PDGFRβ}$ in mice bearing S180 tumor grafts (Arrow indicated). Mice were intravenously injected with CF750-labeled $Z_{PDGFRβ}$ (70 μg/mouse) followed by dynamic scanning using an optical imaging system. Six hours post-injection, the organs and tissues were collected for optical imaging. (For interpretation of the references to colour in this figure legend, the reader is referred to the web version of this article.)

growth suppression in mice bearing B16F1 tumor grafts. However, intravenous injection of 1 μg of *Z*-TNFα showed no apparent tumor growth suppression. The average tumor weight of the mice treated with PBS, 1 μg of Z-TNFα, or 10 μg of *Z*-TNFα was 0.45 ± 0.05 g, 0.37 ± 0.05 g, and 0.17 ± 0.07 g, respectively. The average tumor weight of 10 μg of *Z*-TNFα-treated mice was significantly (P = .012) lighter than that of mice treated with 1 μg of Z-TNFα. The histochemistry analysis revealed obvious cell necrosis in the tumor grafts from mice treated with 10 μg of *Z*-TNFα (Fig. 4C). Further dynamic histological assays demonstrated that numerous red blood cells or clots were observed in tumor grafts collected at 1 h post-injection of 10 μg of *Z*-TNFα (Fig. 4D). Accordingly, the number of dextran particles diffused into the tumor grafts treated with 10 μg of *Z*-TNFα for 1 h was greater than that diffused into the tumor grafts treated with PBS, indicating that an injection of 10 μg of *Z*-TNFα increased vascular permeability (Fig. 4E). However, the bleeding and dextran leakage in *Z*-TNFα-treated tumor grafts were reduced at 4 h post-injection, suggesting thrombosis occurred after hemorrhage. These results indicated that the intravenous injection of high-dose *Z*-TNFα suppressed tumor growth by disrupting tumor vessels and inducing hemorrhagic necrosis.

3.5. *Low-dose Z-TNFα prompts the normalization of tumor vessels in structure and delivery functions*

To investigate whether the intravenous injection of low-dose *Z*-TNFα would prompt the normalization of tumor vessels, mice bearing B16F1 tumor grafts were injected with 1 μg of *Z*-TNFα every other day for a total of three injections. On the second day after the last injection,

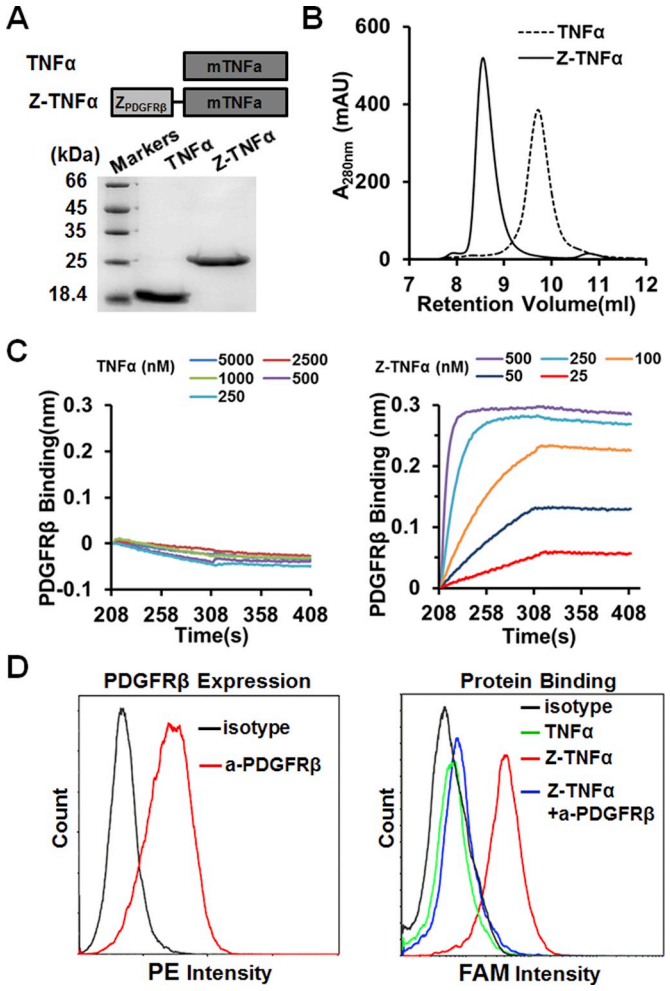

Fig. 3. Preparation and characterization of the fusion protein *Z*-TNFα containing $Z_{PDGFRβ}$ and mouse TNFα (77–233 aa). (A) SDS-PAGE and (B) Size exclusion chromatography of purified *Z*-TNFα and TNFα. (C) Binding of Z-TNFα to PDGFRβ analyzed by biolayer interferometry. PDGFRβ-Fc was immobilized onto a protein A-coated biosensor followed by dipping the biosensor into solutions containing different concentrations of Z-TNFα or TNFα for association and disassociation. (D) PDGFRβ-dependent binding of Z-TNFα to PCs. PDGFRβ expression in PCs was first verified by flow cytometry. To detect the PDGFRβ-dependent cell binding, PCs were preincubated with or without the antibody against PDGFRβ (a-PDGFRβ) prior to the incubation with FAM-labeled *Z*-TNFα.

the structure and function of tumor vessels were examined. As shown in Fig. 5A and Fig. S3, CEUS examination demonstrated that the PI and $AUC_{wash\text{-}in}$ of *Z*-TNFα-treated tumor vessels were significantly ($P < .05$) higher than that of PBS-treated tumor vessels, indicating that the Z-TNFα treatment improved the vascular perfusion of tumor grafts. The TPI of Z-TNFα-treated tumor vessels was shorter than that of PBS-treated tumor vessels. Accordingly, the wash in slope of *Z*-TNFα-treated tumor vessels was higher than that of PBS-treated tumor vessels. These results demonstrated that the *Z*-TNFα-treatment increased the blood flow velocity in tumor grafts. In tumor window model, tumor vessels and blood flow were visualized by intravenously injected FITC-dextran. As shown in Fig. 5B, compared to those in the PBS-treated tumor grafts, the vessels in *Z*-TNFα-treated tumor grafts appeared less tortuous and more homogenous in diameter. Accordingly, the blood flow velocity of Z-TNFα-treated tumor vessels was faster than that of PBS-treated tumor vessels (Supplementary videos). Moreover, the surface area of $CD31^+$ cells was decreased from 16.9 ± 4.2% to 8.5 ± 1.9%, indicating that the number of blood vessels was significantly ($P < .0001$) reduced (Fig. 5C). Moreover, after treatment with *Z*-TNFα, the ratio of $PDGFRβ^+$ cells to $CD31^+$ cells in the tumor grafts was drastically ($P = .0002$) increased from 34.3 ± 6.6% to 70.0 ± 8.5% (Fig. 6A, Fig. S4). Further analysis revealed that the ratios of both $NG2^+$ PCs (Fig. 6B, Fig. S5) and α-SMA^+ SMCs (Fig. 6C, Fig. S6) to $CD31^+$ ECs in *Z*-TNFα-treated tumor grafts were significantly ($P < .0001$) increased (from 29.6 ± 6.2% to 61.6 ± 6.3% for $NG2^+$ cells, and from 9.3 ± 1.6% to 51.4 ± 7.9% for α-SMA^+ cells), indicating that the *Z*-TNFα treatment increased the coverage of PCs and SMCs on tumor vessels. These results demonstrated that the low-dose *Z*-TNFα treatment remodeled tumor vessels as less tortuous, more homogenous in diameter, and increased the mural cell coverage, representing the normalization of the structure of tumor vessels.

To evaluate the function of remodeled tumor vessels, perfusion assays were performed using EC-binding tomato lectin. The proportion of lectin-binding ECs in *Z*-TNFα-treated tumor grafts was 75.3 ± 7.3%, compared to 19.6 ± 2.3% in PBS-treated tumor grafts (Fig. 7A, Fig. S7). These results indicated that the Z-TNFα treatment significantly improved vessel perfusion of tumor. Accordingly, the leakage of dextran assays demonstrated that the surface area of dextran diffused into the tumor tissues was decreased from 6.9 ± 1.1% to 0.5 ± 0.2% after treatment with Z-TNFα (Fig. 7B), indicating that the Z-TNFα treatment improved vessel integrity and reduced vessel permeability. The PIMO area that is proportional to hypoxia was decreased from 15.8 ± 1.8% to 1.7 ± 0.3% (Fig. 7C). Tumor uptake of DOX was increased from 3.8 ± 0.8% to 13.6 ± 0.9% (Fig. 7D, Fig. S8) at 45 min post-injection, reflecting the improvement of tumor vessels in the delivery of oxygen and chemical drugs. These results demonstrated that low-dose *Z*-TNFα treatment prompted the normalization of tumor vessel function.

3.6. Low-dose Z-TNFα improves the antitumor effect of doxorubicin

Since the *Z*-TNFα-mediated vessel normalization facilitated the delivery of antitumor drug DOX into the tumor tissues, we further evaluated the synergetic antitumor effect of *Z*-TNFα and DOX. Considering the nonspecific toxicity of DOX, we first determined the proper dosage of DOX for the combination therapy with *Z*-TNFα. Mice bearing S180 tumor grafts were injected with 1 μg of Z-TNFα followed by the injection of different dosages (1–4 mg/kg) of DOX 2 h later, which was repeated every other day. The tumor volumes and body weight of mice were measured every day. On the second day after the last injection, the tumor grafts were collected and weighed. As shown in Fig. 8A, the antitumor effects of these combination therapies increased with increasing DOX. Although the average tumor weight of mice treated with 4 mg/kg DOX (DOX-4) was lighter, but not significant (0.19 ± 0.06 g vs. 0.31 ± 0.18 g, $P = .12$), than that of mice treated with 3 mg/kg DOX (DOX-3), 4 mg/kg DOX induced a greater weight loss than that did the 3 mg/kg DOX. Consequently, 3 mg/kg DOX was chosen for the combination therapy with *Z*-TNFα in the subsequent experiments.

The synergetic antitumor effect of *Z*-TNFα (1 μg/mouse) and DOX (3 mg/kg) was evaluated in mice bearing S180 or B16F1 tumor grafts. As shown in Fig. 8B, compared to that in mice treated with PBS, mice bearing S180 tumor grafts injected with 1 μg of *Z*-TNFα every other day showed no obviously suppressed tumor growth. At the end of the experiment, the average tumor weight of the *Z*-TNFα-treated mice was 0.79 ± 0.1 g, compared to 0.86 ± 0.1 g for the PBS-treated mice, indicating that a low-dose (1 μg/mouse) of *Z*-TNFα had little direct antitumor effect. As a monotherapy, DOX exerted moderate tumor growth suppression. Once combined with Z-TNFα, its tumor growth suppression was enhanced. The average tumor weight of mice treated with DOX combined with *Z*-TNFα was significantly ($P = .03$) smaller than that of mice treated with DOX as a monotherapy (0.2 ± 0.04 g vs. 0.44 ± 0.1 g). Moreover, injection of 1 μg of Z-TNFα did not show obvious tumor growth suppression in mice bearing B16F1 tumor grafts (Fig. 8C). However, the tumor growth suppression mediated by DOX combined with *Z*-TNFα was much greater than that mediated by DOX alone. At the end of the experiment, the average tumor weight of mice

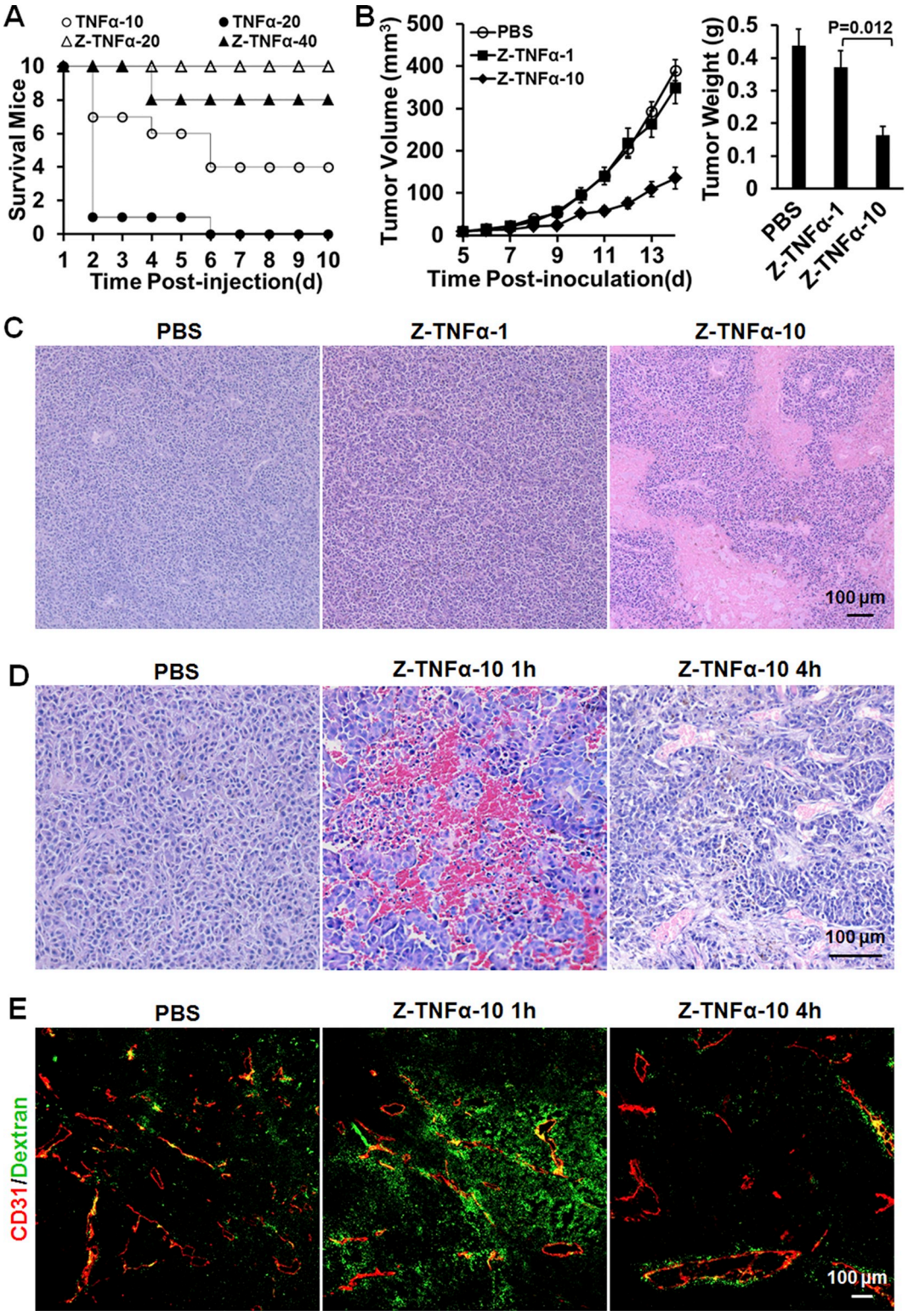

Fig. 4. Antitumor effect of Z-TNFα as monotherapy. (A) Survival of mice treated with Z-TNFα or TNFα. C57BL/6 mice were intravenously injected with *Z*-TNFα (20 or 40 μg/mouse) or TNFα (10 or 20 μg/mouse) every other day three times. The survival of mice was recorded every day. (B) Tumor growth suppression mediated by *Z*-TNFα. Mice bearing B16F1 tumor grafts were intravenously injected with high-dose (10 μg/mouse, Z-TNFα-10) or low-dose (1 μg/mouse, Z-TNFα-1) Z-TNFα every other day beginning on day 5 post-inoculation. PBS was used as the control. The tumor volumes were measured every day. On the second day after the last injection, all tumor grafts were removed and weighed. (C) Histological examination of tumor grafts after treatment with different doses of *Z*-TNFα. (D) Hemorrhage and thrombosis in the tumor grafts early (< 4 h) post-injection of high-dose Z-TNFα. (E) Evaluation of tumor vessel permeability early (< 4 h) post-injection of high-dose *Z*-TNFα. Mice bearing B16F1 tumor grafts were intravenously injected a single dose of *Z*-TNFα (10 μg/mouse). Subsequently, FITC-dextran (1 mg/mouse, green) was intravenously injected at different times post-injection of Z-TNFα. The tumor grafts were removed and sectioned under frozen conditions. The tumor vessels were illustrated by using an antibody against CD31. (For interpretation of the references to colour in this figure legend, the reader is referred to the web version of this article.)

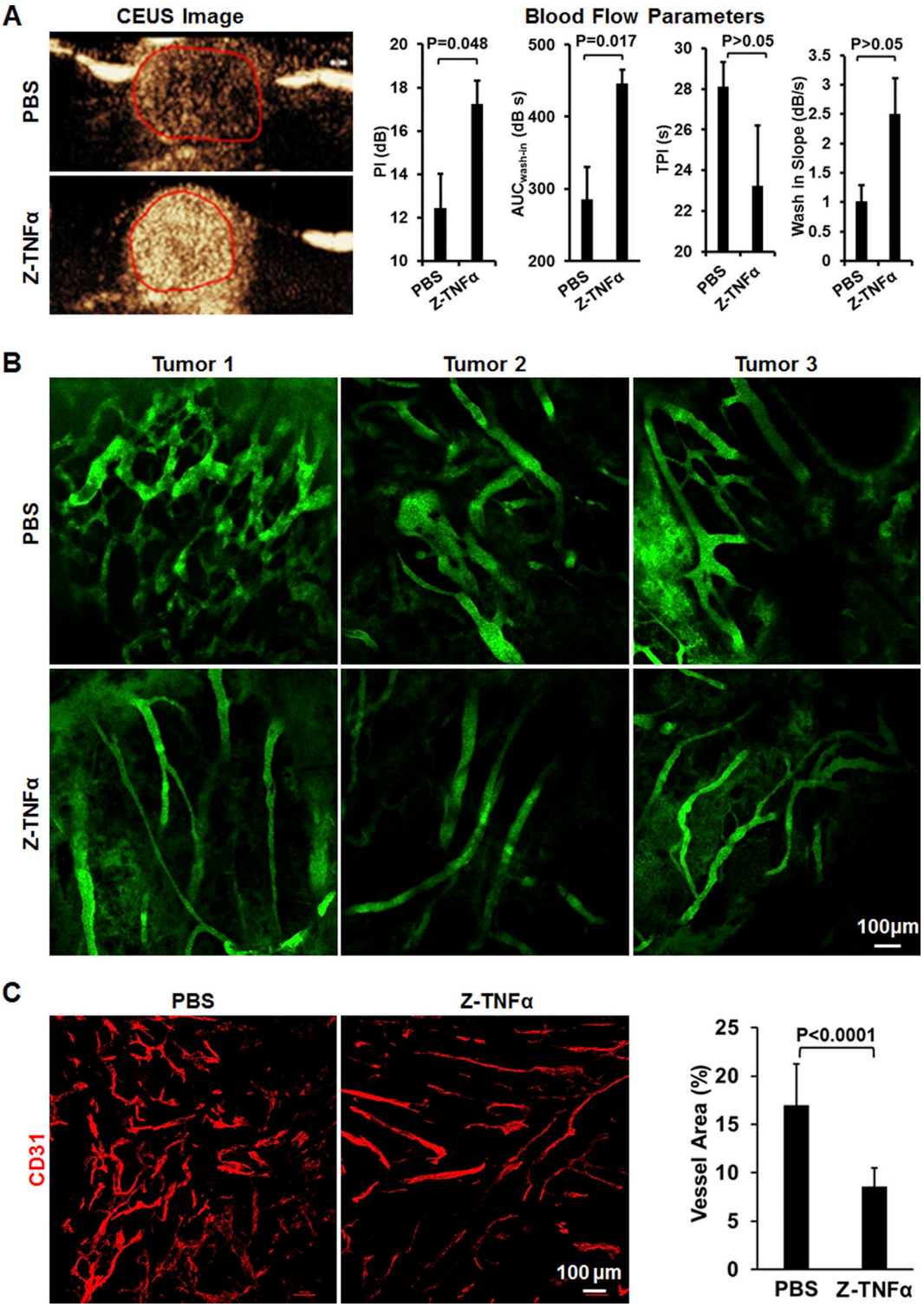

Fig. 5. The *Z*-TNFα treatment changed the function and structure of the tumor vessels. Mice bearing B16F1 tumor grafts were intravenously injected with a low-dose (1 μg/mouse) *Z*-TNFα or PBS every other day three times. (A) Tumor blood flow examined by CEUS. (B) Tumor vessels illustrated by intravenously injected FITC-dextran in tumor window model. (C) Tumor vessels indicated by the $CD31^+$ ECs.

treated with the DOX and *Z*-TNFα combination therapy was significantly ($P = .04$) lighter than that of mice treated with monotherapy of DOX (0.06 ± 0.04 g vs. 0.16 ± 0.09 g). These results demonstrated that low-dose *Z*-TNFα treatment improved the chemotherapy.

Theoretically, Z-TNFα-mediated improvement of chemotherapy might be attributed to synergetic cytotoxicity of *Z*-TNFα and DOX and/or Z-TNFα-mediated enhancement in delivery of DOX. In fact, in vitro assays demonstrated that *Z*-TNFα was not cytotoxic to both S180 and B16F1 tumor cells (Fig. S9A). Although DOX was cytotoxic to S180 and B16F1 tumor cells (Fig. S9B), the combination with *Z*-TNFα did not increase its cytotoxicity in these cells (Fig. S9C). These results suggested that the improvement of the in vivo chemotherapy mediated by Z-TNFα predominantly depends on its role in vessel normalization, which would facilitate the delivery of chemicals into the tumor tissues.

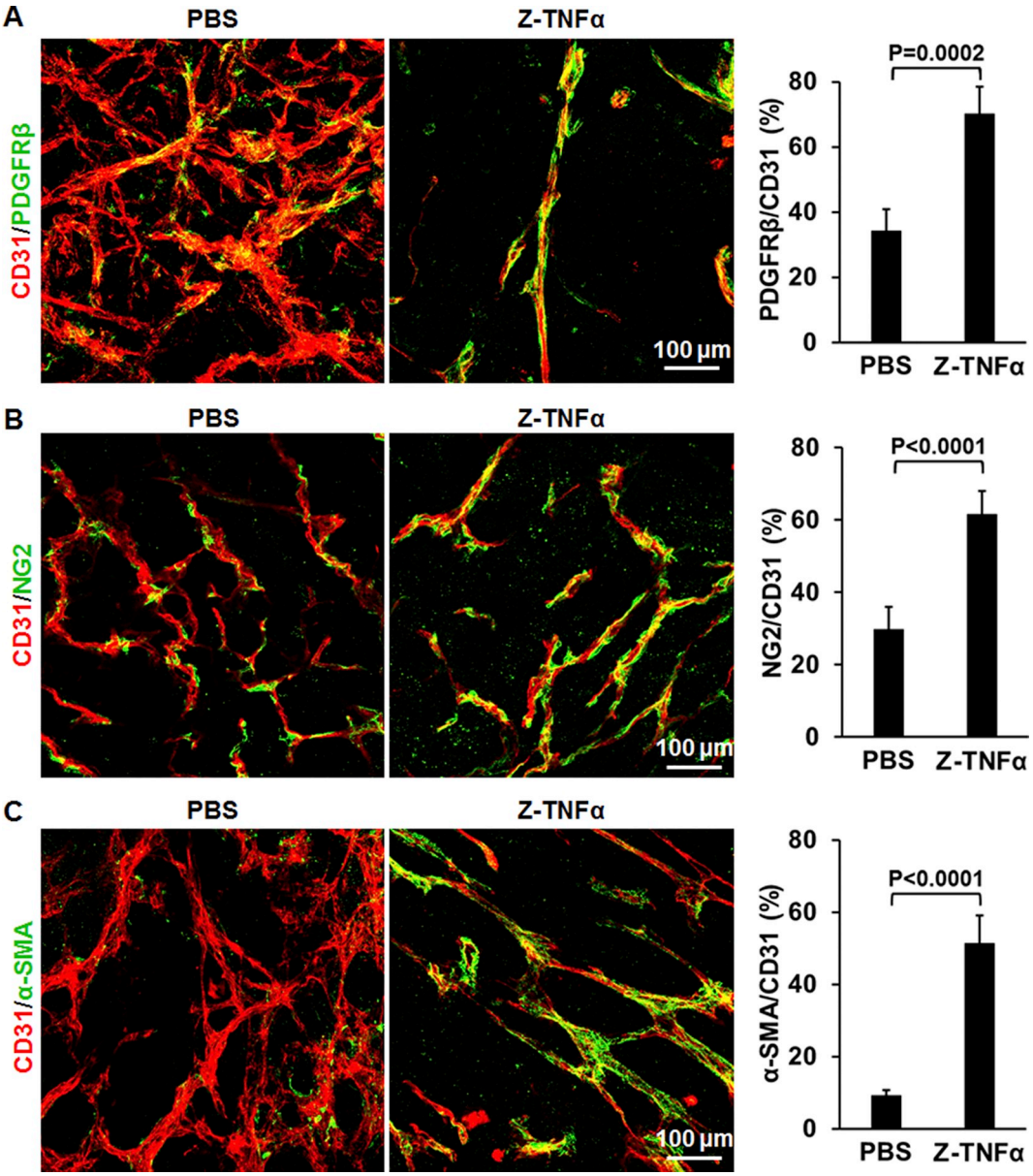

Fig. 6. Low-dose *Z*-TNFα treatment increased the mural cell coverage of tumor vessels. Mice bearing B16F1 tumor grafts were intravenously injected with a low-dose (1 μg/mouse) Z-TNFα or PBS every other day three times. On the second day after the last injection, the tumor grafts were removed and sectioned (100 μm) under frozen conditions. The endothelium was visualized by using an antibody against CD31. The mural cell coverage was reflected by the ratios of PDGFRβ$^+$ (A), NG2$^+$ (B), and α-SMA$^+$ (C) cells to CD31$^+$ ECs in the tumor grafts.

Moreover, unlike the fusion protein *Z*-TNFα comprising of $Z_{PDGFRβ}$ and TNFα, administration of the mixture of unconjugated $Z_{PDGFRβ}$ and TNFα did not improve the antitumor effect of DOX (Fig. 8D), indicating that PC-targeted delivery of TNFα contributed to the tumor vessel normalization.

3.7. Low-dose Z-TNFα treatment altered the function of pericytes

It is known that the PDGF-BB/PDGFRβ pathway involves in VEGF secretion, proliferation and migration of PCs. As an antagonist, $Z_{PDGFRβ}$ could bind and inhibit the phosphorylation of PDGFRβ [26], which might alter the function of PCs. To investigate whether the *Z*-TNFα treatment reduced the secretion of VEGF, PCs were starved overnight followed by the addition of different concentrations of Z-TNFα in the cells. After treatment for 24 h, the medium was collected for quantification of VEGF by ELISA. As shown in Fig. 9A, the stimulation of PCs with PDGF-BB elevated the VEGF concentration from 56.1 ± 5.8 pg/ml to 303.7 ± 14.6 pg/ml. However, the VEGF secreted by PCs treated with *Z*-TNFα, $Z_{PDGFRβ}$, or TNFα were 85.2 ± 8.7, 190.1 ± 5.8, and 260.1 ± 23.3 pg/ml, respectively. These results demonstrated that owing to the fused $Z_{PDGFRβ}$, *Z*-TNFα inhibited VEGF secretion of PCs. Fig. 9B shows that PDGF-BB stimulated the proliferation of PCs, whereas *Z*-TNFα and $Z_{PDGFRβ}$, but not TNFα, neutralized the role of PDGF-BB in cell growth stimulation. The wound-healing assays demonstrated that Z-TNFα and $Z_{PDGFRβ}$, but not TNFα, inhibited the migration of PCs (Fig. 9C). These results demonstrated that Z-TNFα reduced the role of PDGF-BB in stimulating VEGF secretion, proliferation and migration of PCs, which might be predominantly attributed to the fused PDGFRβ-antagonistic $Z_{PDGFRβ}$.

TNFα treatment might upregulate the adhesion molecule that is beneficial for the recruitment of immune cells. As shown in Fig. 9D, Z-TNFα exerted a more potent (positive rate 77.1% vs. 55.6%) induction in ICAM-1 expression in PCs than that exerted by TNFα. Moreover, the perivascular accumulation of tumor-resident macrophages was

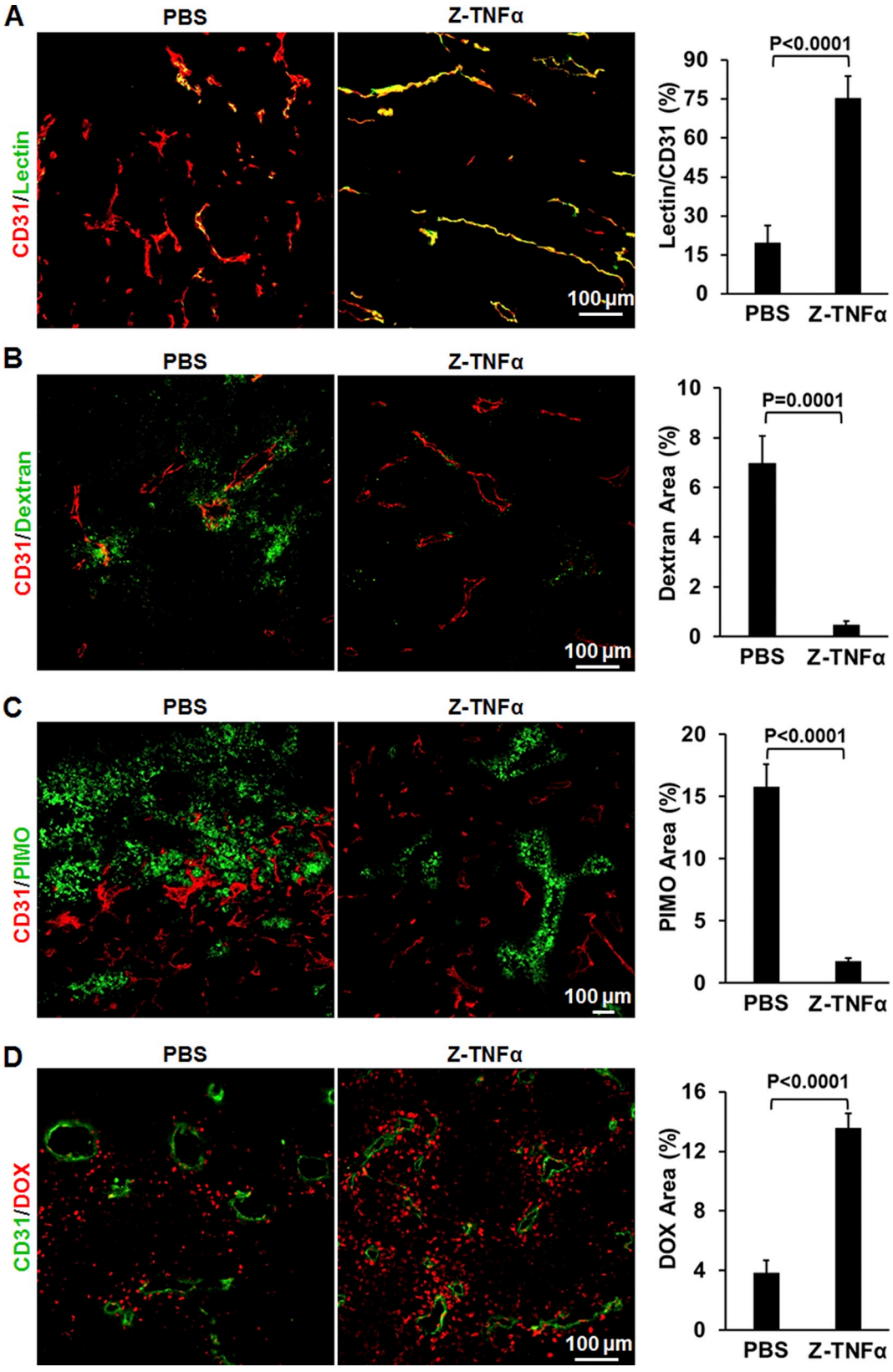

(caption on next page)

observed after treatment with Z-TNFα (Fig. 9E), suggesting that Z-TNFα triggered an interaction between macrophages and PCs that might promote vessel normalization.

3.8. Z-TNFα treatment did not induce obvious acute liver and kidney toxicity

To evaluate the acute liver and kidney toxicity, mice were

Fig. 7. Low-dose Z-TNFα treatment prompts tumor vessel function normalization. Mice bearing B16F1 tumor grafts were intravenously injected with a low-dose (1 μg/mouse) *Z*-TNFα or PBS every other day three times. On the second day after the last injection, the function of the tumor vessels was evaluated. The tumor vessels were indicated by using an antibody against CD31. (A) Perfusion of tumor vessels. After treatments, the mice were intravenously injected with 50 μg of FITC-lectin. Approximately 1.5 h later, heart-perfusions with PBS and 2% PFA were performed prior to the collection of tumor grafts. (B) Permeability of tumor blood vessels. After the treatment, mice were intravenously injected with 1 mg FITC-labeled dextran (70 kDa) followed by 10 min in circulation. The tumor grafts were removed after the heart perfusion. (C) Hypoxia in the tumor grafts. After treatment, mice were intravenously injected with pimonidazole (60 mg/kg) followed by 90 min in circulation. The tumor tissues were stained with the FITC-conjugated anti-Hypoxyprobe-1 antibody (green). (D) Delivery of doxorubicin (DOX) in the tumor grafts. After treatment, mice were intravenously injected with 15 mg/kg doxorubicin. Approximately 45 min later, the tumor grafts were removed and sectioned. (For interpretation of the references to colour in this figure legend, the reader is referred to the web version of this article.)

intravenously injected with low-dose (1 μg/mouse) or high-dose (10 μg/mouse) Z-TNFα or an equal volume of PBS daily for 10 days. The body weights of the mice were recorded every day. All mice were alive during the experiment and their body weights increased with time (Fig. 10A). Nevertheless, high-dose Z-TNFα retarded the growth rate of mice. At the end of the experiment, the function indicator and histology

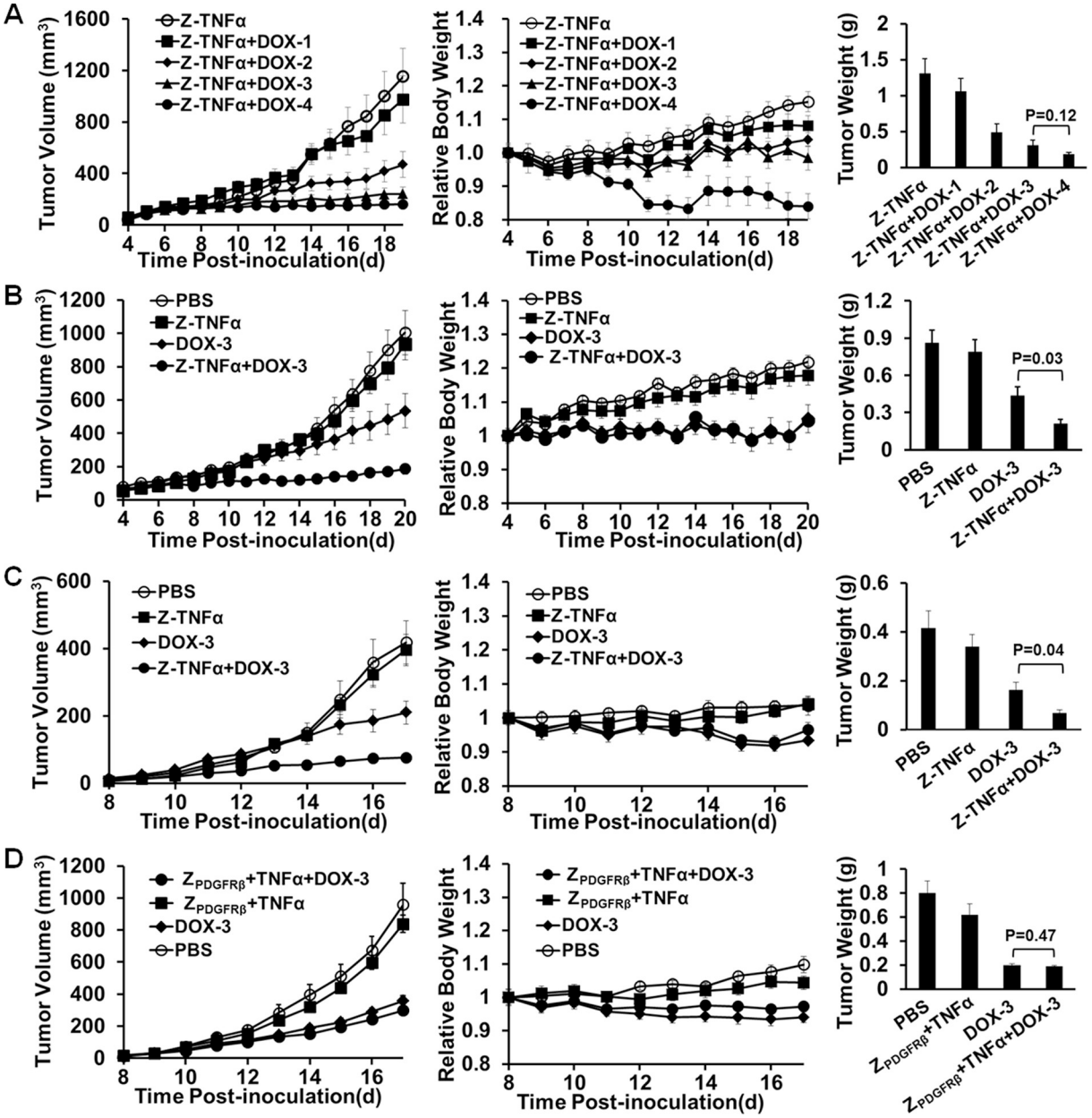

Fig. 8. Low-dose *Z*-TNFα treatment enhances the antitumor effect of doxorubicin (DOX). Mice bearing tumor grafts were intravenously injected Z-TNFα or a mixture of TNFα and $Z_{PDGFRβ}$ followed by intravenous injection of DOX 2 h later. The treatment was performed every other day. The tumor volume and body weight were measured every day. On the second day after the last treatment, all the tumor grafts were removed and weighed. (A) Antitumor effects of different doses (0–4 mg/kg) of doxorubicin in combination with Z-TNFα (1 μg/mouse) treatment. (B, C) Antitumor effects of DOX (3 mg/kg) as monotherapy or in combination with Z-TNFα (1 μg/mouse) in mice bearing S180 (B) or B16F1 (C) tumor grafts. (D) Antitumor effects of DOX (3 mg/kg) as monotherapy or in combination with a mixture of TNFα and $Z_{PDGFRβ}$ in mice bearing B16F1 tumor grafts. The mice were intravenously injected with a mixture of TNFα (0.7 μg/mouse) and $Z_{PDGFRβ}$ (0.3 μg/mouse) followed by an intravenous injection of DOX (3 mg/kg) 2 h later.

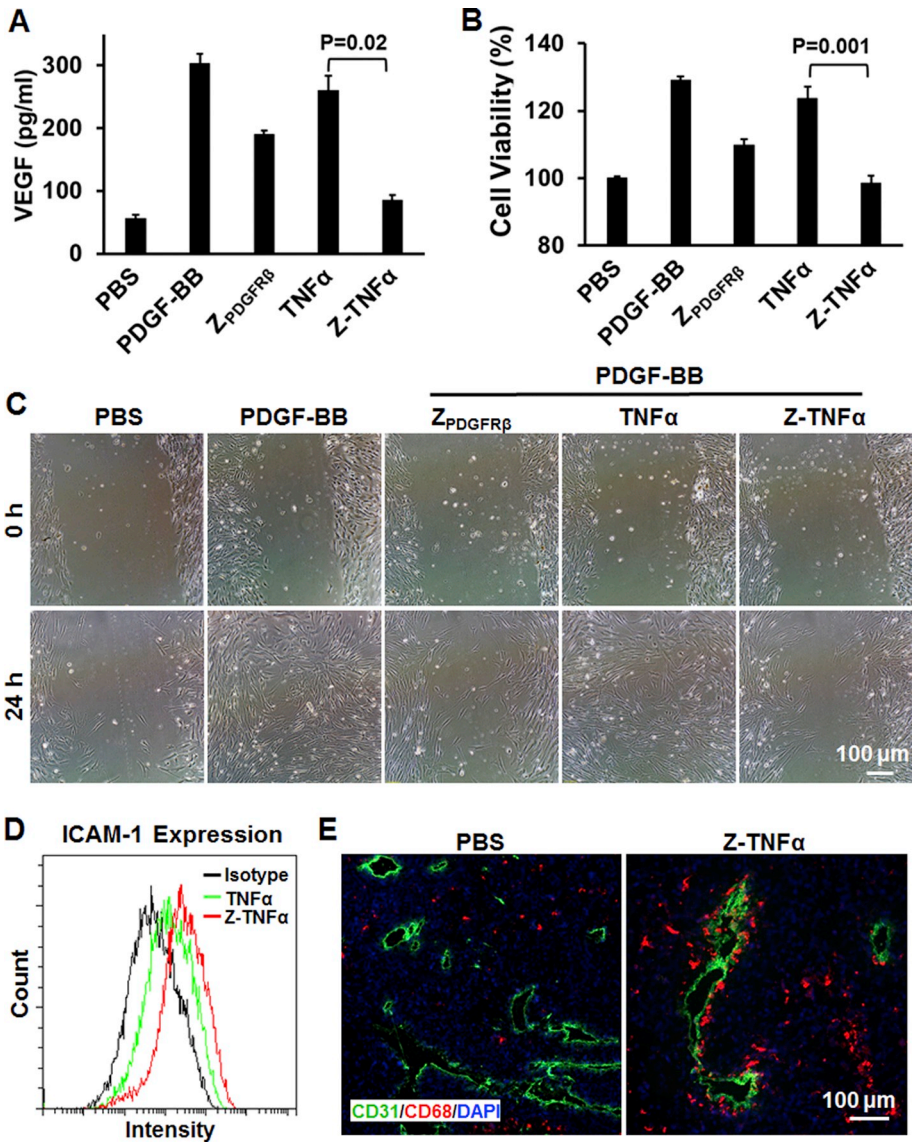

Fig. 9. Regulation of pericyte (PC) function by Z-TNFα. (A) The Z-TNFα treatment reduced VEGF secretion by PCs. PCs (1×10^4 cells/well) starved overnight in 96-cell plates were preincubated with 2.5 nM Z-TNFα, $Z_{PDGFRβ}$, or TNFα for 1 h prior to the addition of 50 ng/ml PDGF-BB. The VEGF in the supernatant of PCs was quantified by ELISA assays. (B) The Z-TNFα treatment suppressed PC proliferation. PCs (8×10^3 cells/well) starved overnight in 96-cell plates were preincubated with 400 nM Z-TNFα, $Z_{PDGFRβ}$, or TNFα for 1 h followed by the addition of 50 ng/ml PDGF-BB. After a 24 h incubation, the cell viability was measured by CCK8. The viability of the cells treated with PBS was considered as 100%. (C) The Z-TNFα treatment inhibited PC migration. PCs (5×10^4 cells/well) were inoculated and starved overnight in 24-cell plates. Scratches were made in the middle of the plate using a 1 ml pipette tip. The cells were preincubated with 200 nM Z-TNFα, $Z_{PDGFRβ}$, or TNFα for 1 h prior to the addition of 50 ng/ml PDGF-BB. The scratches were imaged by phase contrast microscope at 0 and 24 h post-incubation. (D) The Z-TNFα treatment increased ICAM-1 expression in PCs. Detached PCs (1×10^5 cells) were treated with 40 nM Z-TNFα or TNFα. After treatment for 1.5 h on ice, the cells were washed and inoculated in 6-well plates coated with collagen type I. ICAM-1 expression in these cells was analyzed by flow cytometry 24 h later. (E) The Z-TNFα treatment stimulated macrophage attachment to the tumor blood vessels. Mice bearing B16F1 tumor grafts were intravenously injected with Z-TNFα (1 μg/mouse) or PBS every other day three times. On the second day after the last injection, the tumor grafts were sectioned and stained with antibodies against CD68 (red) and CD31 (green). The nuclei of cells were visualized using DAPI (blue). (For interpretation of the references to colour in this figure legend, the reader is referred to the web version of this article.)

of the liver and kidney were examined. As shown in Fig. 10B, the levels of serum AST, ALT, UR, and UA in Z-TNFα-treated mice were similar to those in PBS-treated mice. H&E staining of liver and kidney tissues did not reveal any abnormal structures in the mice treated with low-dose and high-dose *Z*-TNFα (Fig. 10C). These results demonstrated that repeated injections of Z-TNFα had a low risk of nonspecific tissue damage.

4. Discussion

The abnormalities of tumor vessels in their structure and function impaired the blood supply and disabled the infiltration of immune cells and delivery of drugs into tumors. The modulation of tumor-associated vascular cells promoted tumor vessel normalization and increased the response to anticancer chemotherapies and radiotherapies [5,8]. However, the current strategies for vessel normalization predominantly targeted the ECs of tumor vessels directly, which take high risks of damaging the normal vessels during long-term therapy. Modulating ECs indirectly through the mural cells was conceived as a new direction, which might circumvent the problem of the EC-targeted strategy for vessel normalization [23]. As PCs are the major mural cells that regulate ECs and stabilize tumor vessels [34], we chose PCs as the target cells for vessel modulation. It is known that ECs comprise the endothelium, and PCs encompass the endothelial tubule. Owing to the irregularly lined ECs, the endothelium of tumor vessels is usually incomplete, which allows exposure of PCs to drugs in the blood. However, in normal vessels, PCs are covered by the intact endothelium. Compared to the EC-targeted strategies, PC-targeted tumor vasculature modulation theoretically has a lower risk for damaging normal vessels.

To deliver TNFα to PCs, we used the PDGFRβ-specific $Z_{PDGFRβ}$ as a carrier. PDGFRβ is highly expressed in PCs but not in ECs (Fig. 1A). Accordingly, $Z_{PDGFRβ}$ could bind PCs but not ECs (Fig. 2C). In addition to PCs, SMCs also express PDGFRβ. However, few SMCs were observed in the tumor grafts (Fig. 1B). Consequently, intravenously injected $Z_{PDGFRβ}$ distributed predominantly on PDGFRβ$^+$ PCs (Fig. 2D) and accumulated in the tumor grafts (Fig. 2E). TNFα could not bind PDGFRβ, but the $Z_{PDGFRβ}$ fusion endowed TNFα with PDGFRβ- (Fig. 3C) and PDGFRβ$^+$ PC-binding ability (Fig. 3D). PC-binding of *Z*-TNFα was drastically reduced by an antibody against PDGFRβ, indicating that PC-binding of Z-TNFα predominantly depends on PDGFRβ-binding of $Z_{PDGFRβ}$ but not TNFR-binding of TNFα (Fig. 3D). Interestingly, the affinity of the fused $Z_{PDGFRβ}$ in *Z*-TNFα (0.87 nM) for PDGFRβ was approximately 5 times higher than that of the unconjugated $Z_{PDGFRβ}$ (4.5 nM), suggesting that trimeric TNFα-mediated polymerization [35] increased the affinity of the fused $Z_{PDGFRβ}$ for PDGFRβ. Nevertheless, owing to the steric hindrance between the fused domains [36], the N-

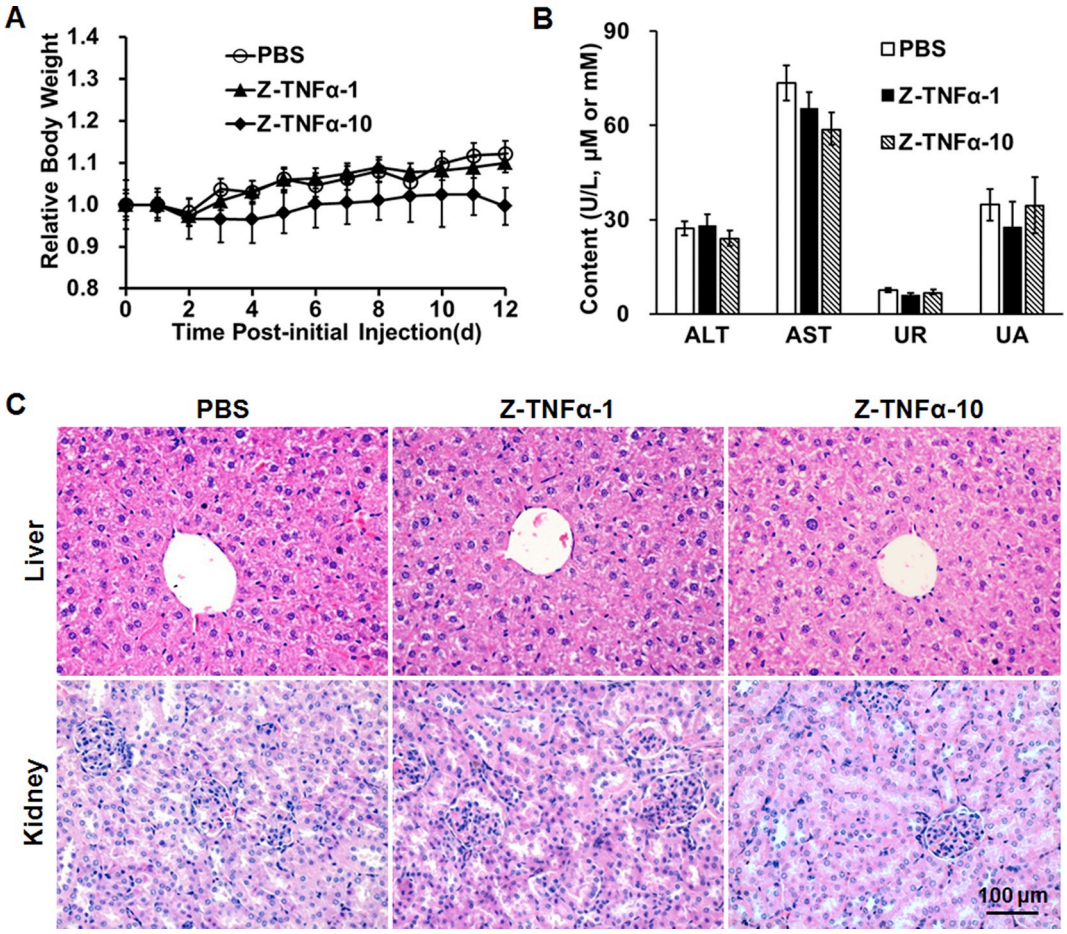

Fig. 10. Acute liver and kidney toxicity of Z-TNFα. ICR mice were intravenously injected with 1 μg/mouse (Z-TNFα-1), 10 μg/mouse (Z-TNFα-10) or PBS every day for ten days. The body weights were measured every day. On the third day after the last injection, the blood, liver and kidney tissues were collected for function and structure analysis. (A) Mouse body weight curves. (B) Biochemical indicators of the liver (ALT and AST) and kidney (Urea and UA) function. (C) H&E staining of the liver and kidney tissues.

terminal fusion of $Z_{PDGFR\beta}$ slightly decreased the affinity of TNFα for TNFR1 and TNFR2 (Fig. S2).

As $Z_{PDGFR\beta}$ fusion reduced the receptor-binding ability of TNFα, the systemic toxicity of the fusion protein *Z*-TNFα was weaker than that of the unconjugated TNFα. The intravenous injection of 20 μg of TNFα induced 90% of mouse death within 24 h, whereas no deaths were observed in mice injected with the same amount of *Z*-TNFα. The injection of 10 μg of TNFα induced 60% mouse mortality (Fig. 4A), whereas the injection of 10 μg of *Z*-TNFα suppressed tumor growth by disrupting tumor vessels but did not induce mouse death (Fig. 4B), suggesting that Z-TNFα could accumulate in the tumor grafts. However, due to the limited sensitivity of the optical imaging system and fluorescence microscope, it is difficult to visualize the tissue and cellular distribution of *Z*-TNFα in the tumor graft when the mice were injected with protein levels lower than 40 μg that might induce the death of mice (Fig. 4A). When the mice were injected with 70 μg of *Z*-TNFα, we examined the tissue and cellular distribution of the protein before the death of the mice. As shown in Fig. S10, optical imaging demonstrated that the uptake of *Z*-TNFα by the tumor was higher than that by normal organs/tissues except for the kidney. Further cellular distribution analysis demonstrated that Z-TNFα was predominantly located on the PDGFRβ$^+$ PCs (Fig. S11). Although the nonspecific distribution of a lethal dose *Z*-TNFα should be considered, these results indicated that TNFα could be delivered to PCs by the $Z_{PDGFR\beta}$ in the tumor vessels.

Similar to current EC-targeted TNFα [17,18], low-dose PC-targeted *Z*-TNFα did not suppress tumor growth in mice (Fig. 4B). However, treatment with low-dose Z-TNFα remodeled the tumor vessels, including reducing the tortuosity (Fig. 5B), increasing the perivascular cell coverage (Fig. 6A, B, and C), enhancing perfusion and blood flow (Fig. 5A, Fig. 7A and supplementary videos), reducing permeability (Fig. 7B) and hypoxia (Fig. 7C). As a result, the low-dose *Z*-TNFα treatment improved the delivery of DOX into tumors (Fig. 7D), suggesting that Z-TNFα might synergize with DOX in anticancer therapy. In fact, DOX combined with Z-TNFα exerted greater tumor growth suppression than that exerted by DOX alone (Fig. 8A, B, and C), which might be attributed to synergetic cytotoxicity of *Z*-TNFα and DOX and/or Z-TNFα-mediated enhancement in delivery of DOX. It was found that Z-TNFα did not increase the cytotoxicity of DOX in tumor cells (Fig. S9C), and low-dose Z-TNFα showed little antitumor effect. However, low-dose Z-TNFα treatment modified tumor vessels in their structure and function and was characterized as 'vessel normalization' (Figs. 5, 6, 7, and supplementary videos), suggesting that the synergism of *Z*-TNFα and DOX was predominantly attributed to the Z-TNFα-mediated improvement of drug delivery. Further experiments revealed that Z-TNFα containing PDGFRβ-antagonistic affibody inhibited PDGF-BB-stimulated VEGF secreted by PCs (Fig. 9A), which might reduce the proliferation and migration of ECs in the tumor grafts. In fact, CD31$^+$ ECs in the tumor grafts were significantly ($P < .0001$) reduced after the treatment of mice with low-dose Z-TNFα (Fig. 5C). Z-TNFα was nontoxic to vascular cells (Fig. S12), but it suppressed the proliferation and migration of PCs in vitro (Fig. 9B and C). Nevertheless, little variation of NG2$^+$ PCs in the tumor grafts was observed before and after treatment with Z-TNFα in vivo (data not shown). Consequently, the increased ratio of PCs to ECs reflecting PC coverage of vessels was

predominantly attributed to the reduction of ECs in the tumors treated with Z-TNFα.

In addition to reducing the VEGF in the tumor microenvironment, triggering the interaction between tumor-resident immune cells and vascular cells also contributes to vessel normalization. As a major component of the tumor stroma, perivascular macrophages were considered the key immune cells involved in vessel normalization [15,18,20,37]. In fact, expression of ICAM-1 in PCs was elevated by *Z*-TNFα (Fig. 9D) and macrophages clustered around the tumor vessels were observed in the tumor grafts after treatment with *Z*-TNFα (Fig. 9E). According to the suggestion by studies on EC-targeted TNFα [17,18], Z-TNFα was supposed to recruit macrophages to the tumor vessels by upregulated ICAM-1 in PCs. In addition to macrophages, T cells were also reported to be involved in vessel normalization [14,17,18,38]. In fact, we examined the $CD4^+$ and $CD8^+$ T cells in the tumor grafts treated after *Z*-TNFα. It was found that both $CD4^+$ and $CD8^+$ T cells in tumor grafts were similar in cell number and distribution before and after treatment with Z-TNFα (Fig. S13), suggesting that T cells contributed little to the vessel normalization mediated by Z-TNFα.

In contrast to Z-TNFα, the mixture of unconjugated $Z_{PDGFR\beta}$ and TNFα did not enhance the anticancer effect of DOX (Fig. 8D), suggesting that the mixture was ineffective for tumor vessel normalization. According to our experiment, both $Z_{PDGFR\beta}$-mediated VEGF reduction and TNFα-mediated immune cells recruitment contributed to vessel normalization mediated by *Z*-TNFα. Although unconjugated $Z_{PDGFR\beta}$ could reduce VEGF secretion and migration of PCs (Fig. 9 A and C), $Z_{PDGFR\beta}$-based monotherapy (60 μg/mouse) showed little effect on tumor vessel normalization (Fig. S14). In addition, TNFα could not bind PDGFRβ+ PCs (Fig. 3D). However, the affinity for PDGFRβ of the fused $Z_{PDGFR\beta}$ was 5 times higher than that of unconjugated $Z_{PDGFR\beta}$. And conjugated TNFα could be delivered to PCs by fused $Z_{PDGFR\beta}$ thus exerted dual hits on PCs. Consequently, the *Z*-TNFα-mediated PCs modulation must be greater than that mediated by the mixture of $Z_{PDGFR\beta}$ and TNFα. This might be an important reason for why the fusion protein *Z*-TNFα, but not the mixture of $Z_{PDGFR\beta}$ and TNFα, efficiently prompted vessel normalization thus enhance the delivery and antitumor effect of combined DOX.

Until now, little is known about the molecular pathways involved in tumor vessel normalization triggered by EC-targeted cytokines, although TGFβ was suggested to be involved in the interaction between macrophages and vascular cells mediated by targeted LIGHT [20,23]. Nevertheless, current EC-targeted TNFα treatments are promising in promoting vessel normalization and improving chemotherapy [22]. Moreover, the immune responses triggered by the EC-targeted TNFα during vessel normalization might break the immunosuppressive microenvironment and enhance the therapeutic efficacy of immune checkpoint blocker [39]. These results demonstrated that the EC-targeted TNFα might be developed as an essential tool for combination anticancer therapy. Currently, EC-targeted TNFα comprises RGD, NGR, or RGR peptides containing one or more Cys residuals that might produce heterogeneous fusion proteins by forming undesired disulfide bridge [22]. However, $Z_{PDGFR\beta}$ contains no Cys residual [26], thus *Z*-TNFα exists as homogenous proteins in solution (Fig. 3B), which might potentiate its clinical application. In addition to the EC-targeted TNFα, the PC-targeted Z-TNFα might be developed as a novel tool for tumor vessel normalization as well as for cancer combination therapy.

5. Conclusions

TNFα could be delivered to tumor-associated $PDGFR\beta^+$ PCs via fused PDGFRβ-agonistic $Z_{PDGFR\beta}$. Low-dose treatment with the fusion protein *Z*-TNFα comprising $Z_{PDGFR\beta}$ and TNFα normalized tumor vessel structure and function, which might have been predominantly attributed to reducing VEGF secretion by PCs, elevating ICAM-1 expression and recruiting macrophages to the tumor vessels. Finally, the low-dose Z-TNFα treatment improved drug delivery and chemotherapy. We conclude that tumor-associated PCs could be considered novel target cells for vessel modulation, and *Z*-TNFα might be developed as a potential tool for anticancer combination therapy.

Supplementary data to this article can be found online at https://doi.org/10.1016/j.jconrel.2019.03.018.

Acknowledgment

This study was funded by the National Natural Science Fund of China (81573336, LXF) and "1.3.5 project for disciplines of excellence, West China Hospital, Sichuan University" (ZYGD18014, CJQ).

Conflict of interests

The authors declare that they have no conflict of interest.

Ethical approval

All applicable institutional guidelines for the care and use of animals were followed.

References

[1] P. Carmeliet, R.K. Jain, Molecular mechanisms and clinical applications of angiogenesis, Nature 473 (2011) 298–307.
[2] K. El Alaoui-Lasmaili, B. Faivre, Antiangiogenic therapy: markers of response, "normalization" and resistance, Crit. Rev. Oncol. Hematol. 128 (2018) 118–129.
[3] S. Azzi, J.K. Hebda, J. Gavard, Vascular permeability and drug delivery in cancers, Front. Oncol. 3 (2013) 211.
[4] B. Theek, M. Baues, F. Gremse, R. Pola, M. Pechar, I. Negwer, K. Koynov, B. Weber, M. Barz, W. Jahnen-Dechent, G. Storm, F. Kiessling, T. Lammers, Histidine-rich glycoprotein-induced vascular normalization improves EPR-mediated drug targeting to and into tumors, J. Control. Release 282 (2018) 25–34.
[5] A.R. Cantelmo, A. Pircher, J. Kalucka, P. Carmeliet, Vessel pruning or healing: endothelial metabolism as a novel target? Expert Opin. Ther. Targets 21 (2017) 239–247.
[6] F.L. Hurwitz, W. Novotny, T. Cartwright, J. Hainsworth, W. Heim, J. Berlin, A. Baron, S. Griffing, E. Holmgren, N. Ferrara, G. Fyfe, B. Rogers, R. Ross, F. Kabbinavar, Bevacizumab plus irinotecan, fluorouracil, and leucovorin for metastatic colorectal cancer, N. Engl. J. Med. 350 (2004) 2335–2342.
[7] A.C. Begg, F.A. Stewart, C. Vens, Strategies to improve radiotherapy with targeted drugs, Nat. Rev. Cancer 11 (2011) 239–253.
[8] R.K. Jain, Antiangiogenesis strategies revisited: from starving tumors to alleviating hypoxia, Cancer Cell 26 (2014) 605–622.
[9] J. RK, Normalizing tumor vasculature with anti-angiogenic therapy: a new paradigm for combination therapy, Nat. Med. 7 (2001) 987–989.
[10] J. Folkman, Angiogenesis, Annu. Rev. Med. 57 (2006) 1–18.
[11] M. Arjaans, C.P. Schröder, S.F. Oosting, U. Dafni, J.E. Kleibeuker, de Vries, EG, VEGF pathway targeting agents, vessel normalization and tumor drug uptake from bench to bedside, Oncotarget 7 (2016) 21247–21258.
[12] J.S. Park, I.K. Kim, S. Han, I. Park, C. Kim, J. Bae, S.J. Oh, S. Lee, J.H. Kim, D.C. Woo, Y. He, H.G. Augustin, I. Kim, D. Lee, G.Y. Koh, Normalization of tumor vessels by Tie2 activation and Ang2 inhibition enhances drug delivery and produces a favorable tumor microenvironment, Cancer Cell 30 (2016) 953–967.
[13] A.R. Cantelmo, L.C. Conradi, A. Brajic, J. Goveia, J. Kalucka, A. Pircher, et al., Inhibition of the glycolytic activator PFKFB3 in endothelium induces tumor vessel normalization, impairs metastasis, and improves chemotherapy, Cancer Cell 30 (2016) 968–985.
[14] L. Tian, A. Goldstein, H. Wang, H. Ching Lo, I. Sun Kim, T. Welte, K. Sheng, L.E. Dobrolecki, X. Zhang, N. Putluri, T.L. Phung, S.A. Mani, F. Stossi, A. Sreekumar, M.A. Mancini, W.K. Decker, C. Zong, M.T. Lewis, X.H. Zhang, Mutual regulation of tumour vessel normalization and immunostimulatory reprogramming, Nature 544 (2017) 250–254.
[15] M. Jarosz-Biej, N. Kaminska, S. Matuszczak, T. Cichon, J. Pamula-Pilat, J. Czapla, R. Smolarczyk, D. Skwarzynska, K. Kulik, S. Szala, M1-like macrophages change tumor blood vessels and microenvironment in murine melanoma, PLoS One 13 (2018) e0191012.
[16] O.E.M. Dirkx AE, M.J. Kuijpers, S.T. van der Niet, V.V. Heijnen, J.C. Bouma-ter Steege, J. Wagstaff, A.W. Griffioen, Tumor angiogenesis modulates leukocyte-vessel wall interactions in vivo by reducing endothelial adhesion molecule expression, Cancer Res. 63 (2003) 2322–2329.
[17] A. Calcinotto, M. Grioni, E. Jachetti, F. Curnis, A. Mondino, G. Parmiani, A. Corti, M. Bellone, Targeting TNF-alpha to neoangiogenic vessels enhances lymphocyte infiltration in tumors and increases the therapeutic potential of immunotherapy, J. Immunol. 188 (2012) 2687–2694.
[18] A. Johansson, J. Hamzah, C.J. Payne, R. Ganss, Tumor-targeted TNFα stabilizes tumor vessels and enhances active immunotherapy, Proc. Natl. Acad. Sci. U. S. A.

109 (2012) 7841–7846.
[19] G.A. Curnis, A. Sacchi, R. Longhi, A. Corti, Coupling tumor necrosis factor-alpha with alphaV integrin ligands improves its antineoplastic activity, Cancer Res. 64 (2004) 565–571.
[20] A. Johansson-Percival, Z.J. Li, D.D. Lakhiani, B. He, X. Wang, J. Hamzah, R. Ganss, Intratumoral LIGHT restores pericyte contractile properties and vessel integrity, Cell Rep. 13 (2015) 2687–2698.
[21] A. Johansson-Percival, B. He, Z.J. Li, A. Kjellen, K. Russell, J. Li, I. Larma, R. Ganss, De novo induction of intratumoral lymphoid structures and vessel normalization enhances immunotherapy in resistant tumors, Nat. Immunol. 18 (2017) 1207–1217.
[22] A. Corti, F. Curnis, G. Rossoni, F. Marcucci, V. Gregorc, Peptide-mediated targeting of cytokines to tumor vasculature: the NGR-hTNF example, BioDrugs 27 (2013) 591–603.
[23] M. Ehling, M. Mazzone, Vessel normalization in the spot-LIGHT of cancer treatment, Trends Mol. Med. 22 (2016) 85–87.
[24] A. Geevarghese, I.M. Herman, Pericyte-endothelial crosstalk: implications and opportunities for advanced cellular therapies, Transl. Res. 163 (2014) 296–306.
[25] J. Ruan, M. Luo, C. Wang, L. Fan, S.N. Yang, M. Cardenas, H. Geng, J.P. Leonard, A. Melnick, L. Cerchietti, K.A. Hajjar, Imatinib disrupts lymphoma angiogenesis by targeting vascular pericytes, Blood 121 (2013) 5192–5202.
[26] M. Lindborg, E. Cortez, I. Hoiden-Guthenberg, E. Gunneriusson, E. von Hage, F. Syud, M. Morrison, L. Abrahmsen, N. Herne, K. Pietras, F.Y. Frejd, Engineered high-affinity affibody molecules targeting platelet-derived growth factor receptor beta in vivo, J. Mol. Biol. 407 (2011) 298–315.
[27] Z. Tao, H. Yang, Q. Shi, Q. Fan, L. Wan, X. Lu, Targeted delivery to tumor-associated pericytes via an affibody with high affinity for PDGFRbeta enhances the in vivo antitumor effects of human TRAIL, Theranostics 7 (2017) 2261–2276.
[28] L.D. McGurn, M. Moazami-Goudarzi, S.A. White, T. Suwal, B. Brar, J.Q. Tang, G.S. Espie, M.S. Kimber, The structure, kinetics and interactions of the beta-carboxysomal beta-carbonic anhydrase, CcaA, Biochem. J. 473 (2016) 4559–4572.
[29] Y. Xi, M. Chen, X. Liu, Z. Lu, Y. Ding, D. Li, CP-673451, a platelet-derived growth-factor receptor inhibitor, suppresses lung cancer cell proliferation and migration, Onco. Targets Ther. 7 (2014) 1215–1221.
[30] D. Wei, Q. Fan, H. Cai, H. Yang, L. Wan, L. Li, X. Lu, CF750-A33scFv-fc-based optical imaging of subcutaneous and orthotopic xenografts of GPA33-positive colorectal cancer in mice, Biomed. Res. Int. (2015) 2015.
[31] Q. Shi, Z. Tao, H. Yang, Q. Fan, D. Wei, L. Wan, X. Lu, PDGFRβ-specific affibody-directed delivery of a photosensitizer, IR700, is efficient for vascular-targeted photodynamic therapy of colorectal cancer, Drug Deliv 24 (2017) 1818–1830.
[32] F. Maione, S. Capano, D. Regano, L. Zentilin, M. Giacca, O. Casanovas, F. Bussolino, G. Serini, E. Giraudo, Semaphorin 3A overcomes cancer hypoxia and metastatic dissemination induced by antiangiogenic treatment in mice, J. Clin. Invest. 122 (2012) 1832–1848.
[33] N. Lassau, M. Chebil, L. Chami, S. Bidault, E. Girard, A. Roche, Dynamic contrast-enhanced ultrasonography (DCE-US): a new tool for the early evaluation of anti-angiogenic treatment, Target. Oncol. 5 (2010) 53–58.
[34] K.D. Barlow, A.M. Sanders, S. Soker, S. Ergun, L.J. Metheny-Barlow, Pericytes on the tumor vasculature: jekyll or hyde? Cancer Microenviron. 6 (2013) 1–17.
[35] H. Liu, L. Dai, Z. Hao, W. Huang, Q. Yang, Hydrophobic cavity in C-terminus is essential for hTNF-alpha trimer conformation, Biochimie 94 (2012) 1001–1008.
[36] I. Fonda, M. Kenig, V. Gaberc-Porekar, P. Pristovaek, V. Menart, Attachment of histidine tags to recombinant tumor necrosis factor-alpha drastically changes its properties, Sci. World J. 2 (2002) 1312–1325.
[37] K.N. Peterson TE, Y. Huang, C.T. Farrar, K.A. Marijt, J. Kloepper, M. Datta, Z. Amoozgar, G. Seano, K. Jung, W.S. Kamoun, T. Vardam, M. Snuderl, J. Goveia, S. Chatterjee, A. Batista, A. Muzikansky, C.C. Leow, L. Xu, T.T. Batchelor, D.G. Duda, D. Fukumura, R.K. Jain, Dual inhibition of Ang-2 and VEGF receptors normalizes tumor vasculature and prolongs survival in glioblastoma by altering macrophages, Proc. Natl. Acad. Sci. U. S. A. 113 (2016) 4470–4475.
[38] R.N. Schmittnaegel, M. Kadioglu, E. Cassará, A. Wyser Rmili, C. Kiialainen, A. Kienast, Y. Mueller, H.J. Ooi, C.H. Laoui, M. D De Palma, Dual angiopoietin-2 and VEGFA inhibition elicits antitumor immunity that is enhanced by PD-1 checkpoint blockade, Sci. Transl. Med. 9 (2017) (pii: eaak9670).
[39] A.R. Elia, M. Grioni, V. Basso, F. Curnis, M. Freschi, A. Corti, A. Mondino, M. Bellone, Targeting tumor vasculature with TNF leads effector T cells to the tumor and enhances therapeutic efficacy of immune checkpoint blockers in combination with adoptive cell therapy, Clin. Cancer Res. 24 (2018) 2171–2181.